A Novel Drug Delivery System for Pancreatic Cancer Treatment: Tumor Targeting with Doxorubicin Liposome Modified with Chlorotoxin-Fc Protein

Samah Ibrahim Mohamed EL-Ghlban

September, 2014

Graduate School of Natural Science and Technology

(Doctor Course)

OKAYAMA UNIVERSITY

The Dissertation Committee for Samah Ibrahim Mohamed EL-Ghlban certifies that this is the approved version of the following dissertation:

A Novel Drug Delivery System for Pancreatic Cancer Treatment: Tumor Targeting with Doxorubicin Liposome Modified with Chlorotoxin-Fc Protein

Committee:

1- Prof. Masaharu Seno, Supervisor
Lab of Nano-Biotechnology

2- Prof. Takashi Sera

3- Prof. Takashi Ohtsuki

A Novel Drug Delivery System for Pancreatic Cancer Treatment: Tumor Targeting with Doxorubicin Liposome Modified with Chlorotoxin-Fc Protein

By

Samah Ibrahim Mohamed EL-Ghlban

Dissertation

Presented to Graduate School of Natural Science and Technology

OkayamaUniversity

In

Partial Fulfillment of the Requirements for the Degree

Of

Doctor of Philosophy in Engineering

September, 2014

CONTENTS

SUMMARY ..... (4-7)

CHAPTER 1: ***General Introduction*** ..... (9-22)

Introducing MMPs and their roles in cancer

Roles of MMPs in cancer progression MMPs and cancer invasion

MMPs and cancer cell proliferation MMPs and cell adhesion, migration MMPs and angiogenesis

Introducing Chlorotoxin

Source, Toxicity and chemical structure

Liposomal drug delivery systems

REFERENCES..... (23-31)

CHAPTER 2: ***Chlorotoxin-Fc fusion inhibits release of MMP-2 from pancreatic cancer cells.***

ABSTRACT..... (34-34)

1. INTRODUCTION..... (35-37)

2. MATERIALS AND METHODS..... (38-45)

2.1. Cell Culture

2.2. Expression and Purification of M-CTX-Fc

2.3. Preparation of the Conditioned Media for Zymography and western blot

2.4. Gelatin Zymography

2.5. Quantitative real-time PCR (qRT-PCR)

2.6. Biotinylation Assay for the Internalization of M-CTX-Fc

2.7. Western Blotting and Image Analysis

2.8. Confocal Microscopic Observation

CONTENTS

2.9. Cell Proliferation Assay

2.10. Cell Migration Assay

2.11. Statistical Analysis

3. RESULTS…… (46-58)

4. DISCUSSION AND CONCLUSION…….. (59-62)

REFERENCES…… (63-70)

CHAPTER 3: ***Antitumor Effect of Novel Doxorubicin Loaded liposomes Modified with Chlorotoxin-Fc protein Against Human Pancreatic Cancer Cells.***

ABSTRACT ……. (72-72)

1. INTRODUCTION…….. (73-75)

2. MATERIALS AND METHODS……... (76-84)

2.1. Materials

2.2. Cell culture and animals

2.3. Expression and Purification of M-CTX-Fc

2.4. Preparation of liposomes

2.4.1. Preparation of DOX loading liposomes

2.4.2. Preparation of DOX loading liposomes modified with M-CTX-Fc or human IgG

2.5. Characterization of liposomes

2.5.1. Size distribution and zeta potential

2.5.2. Encapsulation efficiency (EE) and loading efficiency (LE)

2.5.3. Measurement of lipid concentration

2.5.4. Quantification of M-CTX-Fc conjugated to the liposome

2.5.4.1. Enzyme-linked immunosorbent assay (ELISA)

2.5.4.2. Western blotting

2.6. DOX accumulation in cells

2.7. Fluorescence detection

2.8. In vitro cytotoxicity assay

2.9. Time dependent inhibition (IT50) assay

2.10. In vivo inhibition of tumor growth and toxicity

2.11. Immunohistochemistry (IHC)

2.12. Statistical Analysis

3. RESULTS AND DISCUSSION …… (85-102)

4. CONCLUSION …….. (103-103)

REFERENCES …….. (104-110)

LIST OF PUBLICATIONS …….. (111-111)

ACHNOWLEDGMENT..... (112-113)

SUMMARY

Cancer is one of the leading causes of disease and mortality worldwide. As a result, the past two decades of biomedical research have yielded an enormous amount of information on the molecular events that take place during carcinogenesis and the signalling pathways participating in cancer progression. The molecular mechanisms of the complex interplay between the tumor cells and the tumor microenvironment play a pivotal role in this process. Studies conducted over more than 40 years have revealed mounting evidence supporting that extracellular matrix remodeling proteinases, such as matrix metalloproteinases (MMPs), are the principal mediators of the alterations observed in the microenvironment during cancer progression. For these purpose, molecules that inhibit matrix metalloproteinase (MMP) activity or induce the expression of their natural inhibitors, the tissue inhibitor of metalloproteinases (TIMPs), are potentially interesting. Many MMP inhibitors have been developed for human clinical trials, but effective candidates have not yet been identified. In vitro studies have demonstrated that the proteolytic degradation of extracellular matrix (ECM) components is a major step in tumor invasion. Among the enzymes involved in ECM degradation, the MMP family that contains at least 25 members of metzincin endopeptidases is the most studied.

These enzymes are able to degrade ECM components. MMPs are further divided into subgroups based on whether the enzyme is either secreted or expressed on the cell surface in a membrane-tethered form; soluble MMPs and membrane type MMPs (MT-MMPs). Soluble MMPs are secreted from cells into the extracellular milieu and can diffuse to distal

sites. Therefore, it is believed that this type of MMP is useful for the degradation of ECM in a wider area. Because collagen IV is one of the major components of the basement membrane, MMP-2, a 72-kDa type IV collagenase, is believed to be of special significance during tumor invasion.

Precisely locating tumors always proves to be difficult. To find a molecule that can specifically bind to tumor cells is the key. Recentlly, chlorotoxin (CTX) has been proved to be able to bind to many kinds of tumor cells. The CTX receptors on the cell surface has been demonstrated to be matrix metalloproteinase-2 (MMP-2). CTX has been found to function in such a manner. This peptide is extracted from scorpion venom and is able to specifically bind many tumor cells, which better displays the invasion margins of tumors, and is emerging as a promising technique in diagnostic imaging and targeted therapy for tumors.

MMPs are overexpressed in a variety of malignant tumors, including brain, pancreas, prostate, ovarian, bladder, and lung, and they act as ECM-remodeling enzymes; therefore, targeting of these molecules in cancer therapy is a promising approach to suppress their malignancy. The PANC-1, the human cell line derived from pancreatic carcinoma, is over-expressing MMP-2. The aims of this study are to reveal the inhibition mechanism of CTX, its relevance to MMP-2 and to develop a DDS with liposome displaying M-CTX-Fc in PANC-1 cells.

In this study, the fusion protein was generated by joining the CTX peptide to the amino terminus of the human IgG-Fc domain without a hinge domain, the monomeric form of chlorotoxin (M-CTX-Fc). The resulting fusion protein was then used to target pancreatic cancer cells (PANC-1) in vitro. M-CTX-Fc decreased MMP-2 release into the media of

PANC-1 cells in a dose-dependent manner. M-CTX-Fc internalization into PANC-1 cells was observed. When the cells were treated with chlorpromazine (CPZ), the internalization of the fusion protein was reduced, implicating a clathrin-dependent internalization mechanism of M-CTX-Fc in PANC-1 cells. We also observed colocalization of M-CTX-Fc with EEA-1 that corresponds to the preliminary step in the endosomal pathway before transfer to the sorting endosomes. Furthermore, M-CTX-Fc clearly exhibited the inhibition of the migration depending on the concentration. In summary, M-CTX-Fc was shown to inhibit and arrest the cell proliferation machinery without being toxic to the cells.

All these data raise the possibility that M-CTX-Fc could more broadly be used to specifically deliver conjugated cytotoxic drugs to tumors. Thus, it is necessary to evaluate whether the M-CTX-Fc-modified liposomes could target the pancreatic cancer and further increase the antitumor effect via increasing uptake in tumor cells and hence has an antitumor effect on pancreatic cancer.

To realize this strategy, we established the targeted liposomes conjugated to the monomeric form of chlorotoxin (M-CTX-Fc) and entrapped with anticancer drug (DOX). The physicochemical characterization of the novel liposome system presented a satisfactory size of 100 nm with uniform distribution, high encapsulation and adequate drug loading capacity of anti-cancer drug. Cellular association and internalization studies revealed that attachment of M-CTX-Fc onto the liposomal surface enhanced liposome internalization into PANC-1 cells. In vitro cytotoxicity studies proved that the presence of M-CTX-Fc increased the cytotoxicity against PANC-1 cells which is consistent with its maximum uptake. It was clear suggested that M-CTX-Fc could markedly improve the recognition and uptake of liposomes by PANC-1 cells. In BALB/c mice bearing PANC-1 tumor, the

targeting efficiency and antitumor activity of M-CTX-Fc modified liposome were evaluated. The M-CTX-Fc modified liposomes treatment slowed tumor growth more significantly than non-modified liposomes. The immunohistochemical studies showed a decrease in Ki67 and CD31 staining in tumor cells from DOX-SSL-M-CTX-Fc treated mice when compared with DOX-SSL treated mice, which suggests an inhibition of tumor proliferation rate and angiogenesis process associated with tumor growth. All above results meant that the M-CTX-Fc modified liposome did not cause the unexpected side effects and could be used as safe drug carriers.

In summary, the novel observation that DOX-SSL-M-CTX-Fc can inhibit angiogenesis in the animal model suggests a wider utility of DOX-SSL-M-CTX-Fc in both oncology and other diseases of aberrant neovascularization.

CHAPTER 1

General Introduction

GENERAL INTRODUCTION

1. Introducing MMPs and their roles in cancer

Cancer is one of the leading causes of disease and mortality worldwide [1]. As a result, the past two decades of biomedical research have yielded an enormous amount of information on the molecular events that take place during carcinogenesis and the signalling pathways participating in cancer progression. The molecular mechanisms of the complex interplay between the tumor cells and the tumor microenvironment play a pivotal role in this process [2]. Studies conducted over more than 40 years have revealed mounting evidence supporting that extracellular matrix remodeling proteinases, such as matrix metalloproteinases (MMPs), are the principal mediators of the alterations observed in the microenvironment during cancer progression [2, 3].

Matrix metalloproteinases (MMPs) are a large family of calcium-dependent zinc-containing endopeptidases, which are responsible for the tissue remodeling and degradation of the extracellular matrix (ECM), including collagens, elastins, gelatin, matrix glycoproteins, and proteoglycan. MMPs are usually minimally expressed in normal physiological conditions and thus homeostasis is maintained. However, MMPs are regulated by hormones, growth factors, and cytokines, and are involved in ovarian functions. Endogenous MMP inhibitors (MMPIs) and tissue inhibitors of MMPs (TIMPs) strictly control these enzymes. Over-expression of MMPs results in an imbalance between the activity of MMPs and TIMPs that can lead to a variety of pathological disorders [4–8].

The matrix metalloproteinase (MMP) family consists of at least 23 structurally related [9, 10]. The family shares specific functional and structural components, including a hydrophobic signal peptide for secretion, a propeptide domain for enzyme latency, a catalytic domain with a highly conserved zinc binding site and (for the majority of MMPs) a hemopexin-like C-terminal domain (PEX) linked to the catalytic domain via a flexible hinge region (Figure 1A) [9-11]. The PEX domain binds endogenous tissue inhibitors of MMPs (TIMPs) and certain MMP substrates and is involved in MMP activation [9]. TIMPs include four members originally described as inhibitors of MMP activities, which also have biological activities that are independent of MMP inhibition and regulate cell growth, migration, survival and angiogenesis [12-14]. MMPs include membrane-anchored and secreted MMPs. The membrane-anchored MMPs (MTMMPs) are localized at the cell surface by a C-terminal (type I) transmembrane domain or a glycosylphosphatidylinositol anchor (Figure 1B) [11, 13, 15]. MMPs secreted as latent pro-enzymes include collagenases, stromelysins, matrilysins and two gelatinases (A and B) (Figure 1C) [11, 13]. Removal of the prodomain by other proteolytic enzymes (such as serine proteases, furin, plasmin, and others) leads to MMP activation. Under normal physiological conditions, the proteolytic activity of the MMPs is controlled at any of the following three known stages: activation of the zymogens, transcription, and inhibition of the active forms by various tissue inhibitors of MMPs (TIMPs). In pathological conditions this equilibrium is shifted toward increased MMP activity leading to tissue degradation [16, 17]. TIMPs inhibit most of the secreted MMPs [14]. The gelatinases differ from most of the other MMPs in that they have a collagen-binding domain (CBD) within the catalytic domain (Figure 1C). The CBD is

composed of three fibronectin type II repeats and is involved in the binding of collagenous substrates, elastin, fatty acids and thrombospondins [18].

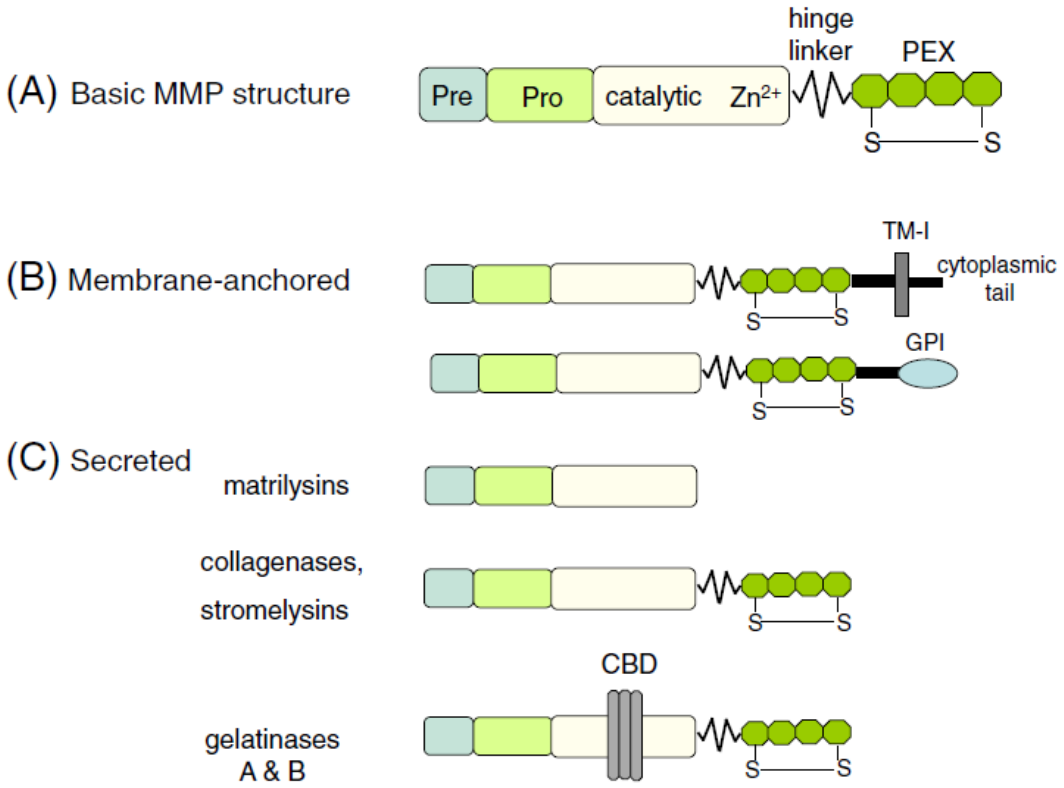

(Brigitte, 2012)

Figure 1. Structures of the MMPs. (A) The general domain structure of MMP family members. The signal peptide (Pre) guides the MMP into the rough endoplasmic reticulum during synthesis. The propeptide domain (Pro) sustains the latency of MMPs. The catalytic domain houses a highly conserved Zn^{2+} binding region. The hemopexin-like-C-terminal domain (PEX) is linked to the catalytic domain by a short hinge region. **(B)** MT-MMPs include membrane-anchored MMPs localized at the cell surface through a C-terminal (type I) transmembrane domain (TM-I) or by a glycosylphosphatidylinositol anchor (GPI). **(C)**

Secreted MMPs include stromelysins, matrilysins, collagenases and gelatinases. The gelatinases (MMP-2 and MMP-9) contain repeats of fibronectin type II-like domains (the collagen binding domain, CBD) that interact with collagen and gelatin.

Matrix metalloproteinases selectively degrade various components of the extracellular matrix (ECM) and release growth factors and cytokines that reside in the ECM [16, 19]. The MMPs are also capable of activating various latent growth factors, cytokines and chemokines and cleaving cell surface proteins (cytokine receptors, cell adhesion molecules, the urokinase receptor, etc.) [9, 10, 17, 20]. Angiogenesis is an invasive process that requires proteolysis of the extracellular matrix and, proliferation and migration of endothelial cells, as well as synthesis of new matrix components. The MMPs are clearly implicated in angiogenesis. Through their proteolytic activity, MMPs play crucial roles in invasion and metastasis and regulate signaling pathways that control cell growth, survival, invasion, inflammation and angiogenesis (figure 2) and (Figure 3].

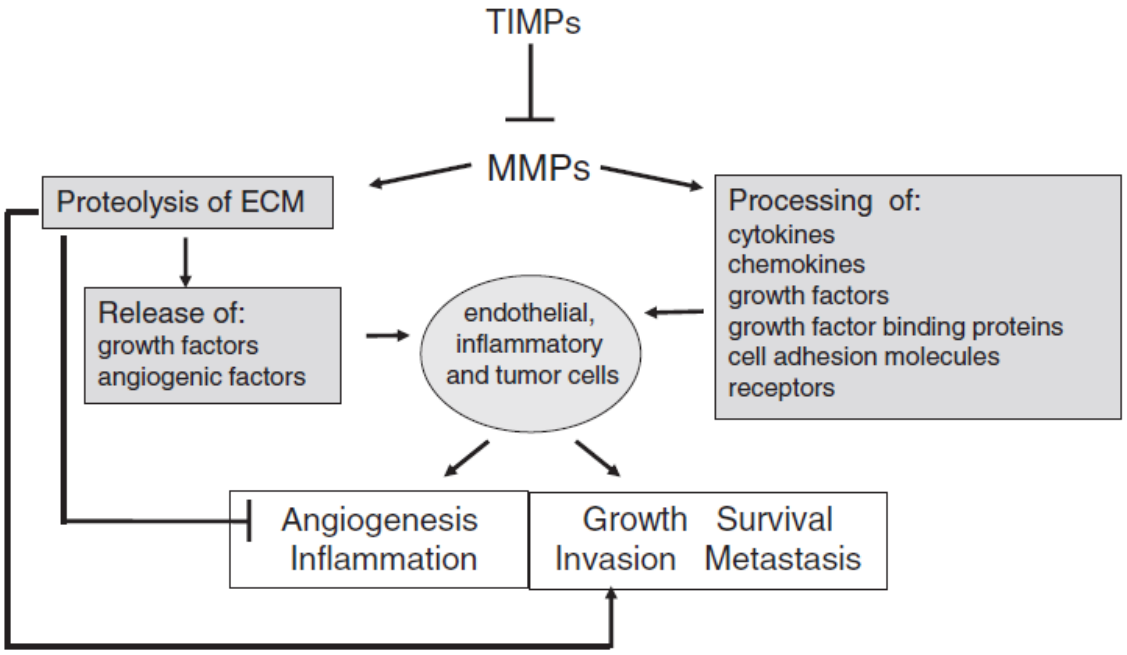

(Brigitte, 2012)

Figure 2. A schematic overview of the roles of MMPs in cancer. MMPs degrade structural components within the ECM, facilitating tumor cell invasion and metastasis and thus releasing growth factors, cytokines and angiogenic factors embedded in the ECM (VEGF, TGF-β, bFGF, IFN-γ, etc.). MMPs also generate angiogenesis inhibitors, such as angiostatin, endostatin and tumstatin. MMPs process and activate or inactivate signaling molecules (cytokines, chemokines, growth factors) that target immune cells (inflammation), endothelial cells (angiogenesis) and tumor cells (cell growth, survival, migration, invasion and metastasis). MMP-mediated cleaving of adhesion molecules (E-cadherin, ICAM-1, integrins, etc.) enhances tumor cell migration and invasion. (⊣ negative regulation, → positive regulation)

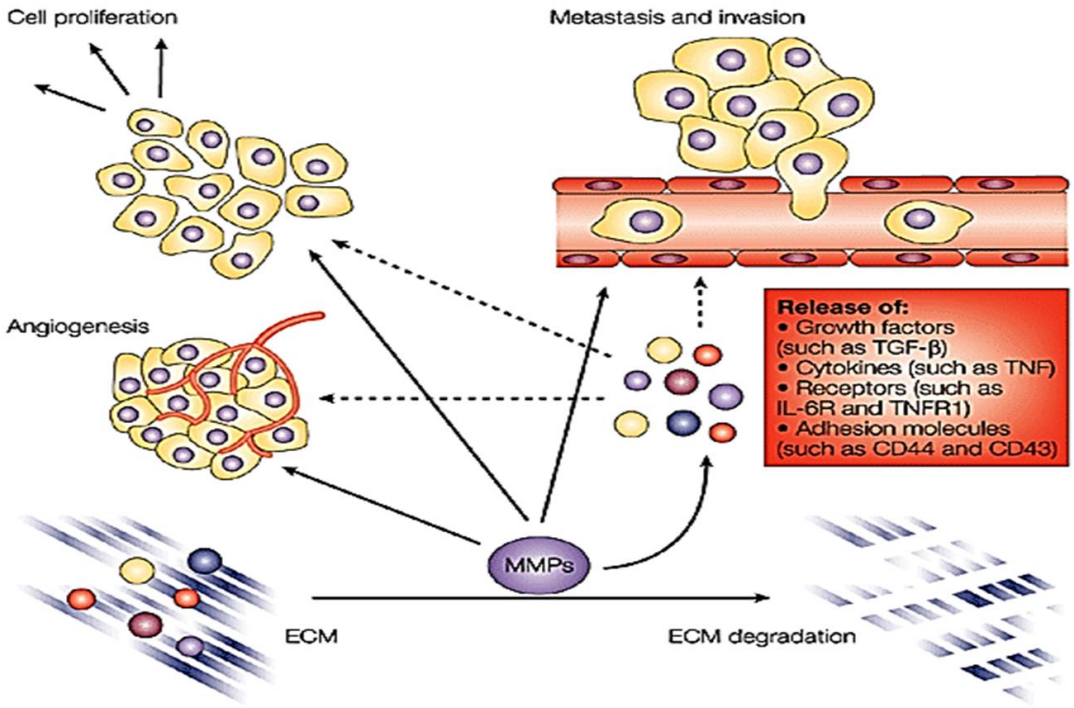

Figure 3. Role of MMPs in cancer.

Roles of MMPs in cancer progression

During development of carcinogenesis, tumor cells participate in several interactions with the tumor microenvironment involving extracellular matrix (ECM), growth factors and cytokines associated with ECM, as well as surrounding cells (endothelial cells, fibroblasts, macrophages, mast cells, neutrophils, pericytes and adipocytes) [21-23]. Four hallmarks of cancer that include migration, invasion, metastasis and angiogenesis are dependent on the surrounding microenvironment. Critical molecules in these processes are MMPs because they degrade various cell adhesion molecules, thereby modulating cell–cell and cell–ECM interactions.

MMPs and cancer cell invasion

The ECM is a dynamic structure that orchestrates the behavior of the cells by interacting with them. The proteolytic activity of MMPs is required for a cancer cell to degrade physical barriers during local expansion and intravasation at nearby blood vessels, extravasation and invasion at a distant location. During invasion, the localization of MMPs to specialized cell surface structures, called invadopodia, is requisite for their ability to promote invasion. These structures represent the site where active ECM degradation takes place. Invadopodia utilize transmembrane invadopodia-related proteinases, including MMP-14 [membranetype MT1-MMP], several members of the ADAM family, as well as secreted and activated MMPs at the site, such as MMP-2 and -9, to degrade a variety of ECM macromolecules and facilitate cell invasion [24].

MMPs and cancer cell proliferation

There are several mechanisms by which MMPs contribute to tumor cell proliferation. In particular, they can modulate the bioavailability of growth factors and the function of cell-surface receptors. Members of the MMP and ADAM families can release the cell-membrane-precursors of several growth factors, such as insulin-like growth factors (IGFs) and the epidermal growth factor receptor (EGFR) ligands that promote proliferation. Several MMPs (MMP-1, -2, -3, -7, -9, -11 and -19) and ADAM12 cleave IGF-binding proteins that regulate the bioavailability of the growth factor [25, 26]. One of the key observations that has emerged from several studies is the pivotal role of the interactions between glycosaminoglycans (GAGs)-MMPs-GFs, leading to the activation of the

proMMPs and their subsequent proliferative effects. Notably, GAGs chains can recruit MMPs to release growth factors from the cell surface and, as a result, induce cancer cell proliferation. For example, MMP-7 exerts high affinity for heparan sulfate chains. On the basis of this notion, heparan sulfate chains on cell surface receptors, such as some variant isoforms of CD44, anchor the proteolytically active MMP-7, resulting in the cleavage of HB-EGF [27].

MMPs and cell adhesion, migration

Cell movement is highly related to the proteolytic activity of MMPs and ADAMs, regulating the dynamic ECM–cell and cell–cell interactions during migration. Initially, the generation of cryptic peptides via degradation of ECM molecules, such as collagen type IV and laminin-5, promotes the migration of cancer cells [28, 29]. Several integrins play an active role in regulation of cell migration because they can serve as substrates for MMPs [30].

MMPs and angiogenesis

MMPs contribute to angiogenesis not only by degrading basement membrane and other ECM components, allowing endothelial cells to detach and migrate into new tissue, but also by releasing ECM-bound proangiogenic factors (bFGF, VEGF, and TGF). In addition, MMP degradation of ECM components generates fragments with now-accessible integrin binding sites, triggering integrin intracellular signaling. By directly binding to αvβ3, MMP-2 may itself initiate integrin signaling and thereby contribute to endothelial

cell survival and proliferation (31). However, MMPs also are able to generate endogenous angiogenesis inhibitors from larger precursors: cleavage of plasminogen by MMPs releases angiostatin; endostatin is the COOH terminal fragment of the basement membrane collagen XVIII, which can be generated by cleavage by cathepsins and MMPs; and generation of the hemopexin domain of MMP-2 from MMP-2 may be through autocatalysis (31, 32). Thus, the MMPs have both pro- and antiangiogenic functions. On the whole, however, MMPs are required for angiogenesis, and MMPIs have been shown to inhibit angiogenesis in animal models (33).

2. Introducing Chlorotoxin

Precisely locating tumors always proves to be difficult. To find a molecule that can specifically bind to tumor cells is the key. Recentlly, egyptian scorpion chlorotoxin (CTX) has been proved to be able to bind to many kinds of tumor cells. The CTX receptors on the cell surface has been demonstrated to be matrix metalloproteinase-2 (MMP-2). Chlorotoxin (CTX) has been found to function in such a manner. This peptide is extracted from scorpion venom and is able to specifically bind many tumor cells, which better displays the invasion margins of tumors, and is emerging as a promising technique in diagnostic imaging and targeted therapy for tumors.

Source, toxicity, and chemical structure

CTX is a 36amino acid peptide extracted from the venom of *Leiurus quinquestriatus* and belongs to the scorpion toxin like superfamily [34]. CTX is a peptide containing 36 amino acids and 4 disulfide bonds at a relative molecular mass of 3950 u, including 1

tyrosine residue, 8 cysteine residues, and 4 disulfide bonds. The tyrosine residue can be labeled with radioactive iodine and the 8 cysteine residues are conjugated through the 4 disulfide bonds [34] .The amino acid sequence of CTX is listed as follows: MCMPCFTTDHQMARKCDDCCGGKGRGKCYGPQCLCR [35]. CTX is highly folded by the four disulfide bonds in its structure. Therefore, it has a smaller volume and more condensed molecular structure, readily delivered through the narrow extracellular matrix [36]. CTX has emerged as a new platform for diagnostic imaging and treatment of tumors, with some major benefits: (1) its smaller and condensed structure; (2) the feasibility of artificial synthesis and the readily modified chemical structure with a tyrosine residue conjugating iodine or other molecules covalently; (3) its ability to penetrate the blood brain barrier and more readily diffuse into tumor parenchymas; (4) it is not readily eliminated through the metabolism with a longer imaging time due to intracellular binding with tumor cells; (5) its derivation from an invertebrate, being not rejected by human tissue, the absence of intimate toxicity without binding to normal tissue and cells; and (6) its antitumor activity in inhibiting tumor invasion and metastasis [34] . Whether CTX specifically binds to tumor cells from other human systems, especially those from MMP2 positive tumors, remains to be verified. Localizing tumor cells with CTX, despite that specifically binds tumor cells, is still difficult. Currently, investigators have conjugated CTX with radioactive iodine isotopes, fluorescent molecules, and nanoparticles, and subsequently localized these conjugants with the imaging tools. However, most tools for localization are defective or complex, and developing a simple and effective localizing method continues to be extensively studied. Additionally, the hazards of various complexes in vivo should be monitored in the long term. The further study on CTX and the

development of its complexes will make it promising for CTX to become a novel modality for diagnosis and targeted therapies for tumor.

Chlorotoxin was shown to inhibit the migration and invasion of glioma cells possibly via the modulation of ion channels (36). Subsequent studies suggested that chlorotoxin modulates the chloride ion channel in glioma cells by facilitating the internalization and, hence, the down-regulation of the cell surface levels of the CLC-3 chloride channel (37). Chlorotoxin was shown to bind a macromolecular complex containing MMP-2, membrane type metalloprotease-1, tissue inhibitor of metalloprotease-2 (38), and the CLC-3 chloride channel at the surface of glioma cells and mediate the internalization and down-regulation of both MMP-2 and CLC-3 (37, 38). Chlorotoxin was also able to inhibit the in vitro activity of MMP-2 and the cell surface gelatinolytic activity in D54-MG cells, supporting an interaction between MMP-2 and chlorotoxin in glioma cells (38). In addition to glioma cells, chlorotoxin has been shown to specifically bind other tumors of neuroectodermal origin (39). Recently, using mouse tumor models, a bio-conjugate of chlorotoxin with the nearly infrared dye Cy5.5 (CTX:Cy5.5) was shown to efficiently detect and monitor multiple tumor types, including glioma, medulloblastoma, prostate cancer, intestinal cancer, and sarcoma following intravenous injection (40). Multifunctional nanoparticles modified with ClTx for the tumor imaging were also investigated.

3. Liposomal drug delivery systems

Nanoliposomes are self-closed colloidal particles in which bilayered membrane(s) composed of self-aggregated lipid molecules make the vesicles. They encapsulate a fraction of the medium in which they are suspended into their interior (41). Liposomal vesicles have

drawn the attention of researchers as potential carriers of various bioactive molecules that could be used for therapeutic applications in both humans and animals (42, 43). Liposomes have been studied as models of biological membranes and more recently as carriers for the introduction of genes and drugs into target cells; (41, 44–47) thus, liposomes have been successful as carriers of antitumor drugs in cancer chemotherapy (48) and for gene delivery purposes (49).

These delivery systems control the distribution of liposome by adjusting its particle size and the electric charge of its surface, and deliver the medicines to the targets, that is, passive delivery systems [50-52]. In addition, so far trials which have given an active targeting ability to the liposome by binding various ligands (antibody, transferrin, folic acid, monosaccharide, etc.) on its surface have been done, but successful cases are few [52, 53]. In recent years, drug delivery research has increasingly focused on antibody-targeting liposomes in the treatment of cancers.

Sterically stabilized polyethyleneglycol (PEG)-modified liposomes have already been optimized for escaping uptake by reticuloendothelial system (RES) and prolonging systemic circulation (54), which resulted in increased accumulation in tumor tissue by enhanced permeation and retention (EPR) effect (55). Targeting of liposomes to specific cells is a promising strategy for reducing side effects and improving therapeutic effects.

Recent progress in cancer physiology revealed that tumor growth is closely related to the development of new blood vessels. Then, inhibition of neovascularity is a potent strategy for cancer therapy. One of the key proteins on angiogenesis in tumor vessels is membrane type-1 matrix metalloproteinase (MT1- MMP), which is expressed on the neovascularity as well as tumor cells. On the plasma membrane, MT1-MMP cleaved

extracellular matrix components such as collagen, laminin, fibronectin and elastin (56-62). Simultaneously, MT1-MMP activates soluble MMPs (i.e. MMP-2) via its proteolytic activity, which also plays an important role in the degradation of the matrix (56, 58, 60-62). In fact, administration of the inhibitors for MMP families to the tumor-bearing mouse suppressed the angiogenesis, which resulted in the antitumor effect (63, 64). Based on previous report, dual targeting of antitumor drugs to the neovascular cells and tumor cells are expected to be excellent strategy for the cancer therapy (65). However, all the studies of ClTx have focused on brain tumors, regardless of the area of tumor diagnosis, gene delivery method and chemical drug delivery method. It remains an open question whether ClTx modified drug delivery system could specifically bind to other tumor cells beside gliomas. Since the ClTx receptor is MMP-2, which is also highly expressed highly expressed in pancreatic cancer, breast cancer, lung cancer and so on. Thus it is necessary, to evaluate whether chlorotoxin modified drug delivery system has anti-tumor effect on pancreatic cancer cells.

REFERENCES

1. Jemal A, Tiwari RC, Murray T, Ghafoor A, Samueis A, Ward E, Feuer EJ and Thum MJ. Cancer statistics. CA Cancer J Clin. 2004; 54: 9–29.
2. Kessenbrock K, Plaks V and Werb Z. Matrix metalloproteinases: regulators of the tumor microenviroment. Cell. 2010; 141: 52–67.
3. Page-McCaw A, Ewald AJ and Werb Z. Matrix metalloproteinases and the regulation of tissue remodelling. Nat Rev Mol Cell Biol. 2007; 8: 221–233.
4. Aranapakam V, Grosu GT, Davis JM, Hu B, Ellingboe J, Baker JL, Skotnicki JS, Zask A, DiJoseph JF, Sung A, Sharr MA, Killar LM, Walter T, Jin G, Cowling R. Synthesis and structure-activity relationship of alpha-sulfonylhydroxamic acids as novel, orally active matrix metalloproteinase inhibitors for the treatment of osteoarthritis. J. Med. Chem. 2003; 46: 2361-2375.
5. Engel CK, Pirard B, Schimanski S, Kirsch R, Habermann J, Klingler O, Schlotte V, Weithmann KU, Wendt KU. Structural basis for the highly selective inhibition of MMP-13. Chem. Biol. 2005; 12: 181-209.
6. Amin EA, Welsh WJ. Three-dimensional quantitative structure-activity relationship (3D-QSAR) models for a novel class of piperazine-based stromelysin-1 (MMP-3) inhibitors: applying a "divide and conquer" strategy J. Med. Chem. 2001; 44: 3849-3855.

7. Raspollini MR, Castiglione F, Degl'Innocenti DR, Garbini F, Coccia ME, Taddei GL. Difference in expression of matrix metalloproteinase-2 and matrix metalloproteinase-9 in patients with persistent ovarian cysts. Steril. 2005; 84: 1049-1052.
8. Venkatesan AM, Davis JM, Grosu GT, Baker J, Zask A, Levin JI, Ellingboe J, Skotnicki JS, DiJoseph JF, Sung A, Jin G, Xu W, McCarthy D J, Barone D. Synthesis and structure-activity relationships of 4-alkynyloxy phenyl sulfanyl, sulfinyl, and sulfonyl alkyl hydroxamates as tumor necrosis factor-alpha converting enzyme and matrix metalloproteinase inhibitors J. Med. Chem. 2004; 47: 6255-6269.
9. Kessenbrock K, Plaks V, Werb Z, Matrix metalloproteinases: regulators of the tumor microenvironment. Cell. 2010; 141: 52–67.
10. Klein T, Bischoff R. Physiology and pathophysiology of matrix metalloproteases. Amino Acids. 2011; 41: 271–290.
11. Brigitte B. New facets of matrix metalloproteinases MMP-2 and MMP-9 as cell surface trasducers: outside-in signalling and relationship to tumor progression. Biochimica et Biophysica Acta. 2012; 29-36.
12. Cruz-Munoz W, Khokha R. The role of tissue inhibitors of metalloproteinases in tumorigenesis and metastasis. Crit. Rev. Clin. Lab. Sci. 2008; 45: 291–338.
13. Bourboulia D, Stetler-Stevenson WG. Matrix metalloproteinases (MMPs) and tissue inhibitors of metalloproteinases (TIMPs): positive and negative regulators in tumor cell adhesion. Semin Cancer Biol. 2010; 20: 161–168.
14. Brew K, Nagase H. The tissue inhibitors of metalloproteinases (TIMPs): an ancient family with structural and functional diversity. Biochim. Biophys. Acta. 2010; 1803: 55–71.

15. Devy L, Dransfield DT. New strategies for the next generation of matrixmetalloproteinase inhibitors: selectively targeting membrane-anchored MMPs with therapeutic antibodies, Biochem. Res. Int. 2011; doi:10.1155/2011/191670.
16. Cheng M, De B, Pikul S, Almstead NG, Natchus MG, Anastasio MV, McPhail SJ, Snider CE, Taiwo YO, Chen L, Dunaway CM, Gu F, Dowty ME, Mieling GE, Janusz MJ, Wang-Weigand S. Design and synthesis of piperazine-based matrix metalloproteinase inhibitors. J. Med. Chem. 2000; 43: 369.
17. Kontogiorgis, CA, Papaioannou P, Hadjipavlou-Litina D. Matrix metalloproteinase inhibitors: a review on pharmacophore mapping and (Q)SARs results. J. Curr. Med. Chem. 2005; 12: 339.
18. Bjorklund M, Koivunen E. Gelatinase-mediated migration and invasion of cancer cells, Biochim. Biophys. Acta. 2005; 1755: 37–69.
19. Roy R, Yang J, Moses MA. Matrix metalloproteinases as novel biomarkers and potential therapeutic targets in human cancer. J. Clin. Oncol. 2009; 27: 5287–5297.
20. Rodriguez D, Morrison CJ, Overall CM. Matrix metalloproteinases: what do they not do? New substrates and biological roles identified by murine models and proteomics. Biochim. Biophys. Acta. 2010; 1803 39–54.
21. Kessenbrock K, Plaks V, and Werb Z. Matrix metalloproteinases: regulators of the tumor microenviroment. Cell. 2010; 141: 52–67.
22. Murphy G. The ADAMs: signalling scissors in the tumour microenvironment. Nat Rev Cancer. 2008; 8: 932–941.
23. Deryugina IE, and Quigley PJ. Matrix metalloproteinases and tumor metastasis. Cancer Metastasis Rev. 2006; 25: 9–34.

24. Weaver MA. Invadopodia: specialized cell structures of cancer invasion. Clin Exp Metastasis. 2006; 23: 97–105.

25. Loechel F, Fox JW, Murphy G, Albrechtsen R and Wewer UM, ADAM 12-S Cleaves IGFBP-3 and IGFBP-5 and is inhibited by TIMP-3. Biochem Biophys Res Commun. 2000; 278: 511–515.

26. Nakamura M, Miyamoto S, Maeda H, Ishii G, Hasebe T, Chiba T, Asaka M, Ochiai A. Matrix metalloproteinase-7 degrades all insulin-like growth factor binding proteins and facilitates insulin like growth factor bioavailability. Biochem Biophys Res Commun. 2005; 333: 1011–1016.

27. Gialeli Ch, Kletsas D, Mavroudis D, Kalofonos HP, Tzanakakis GN and Karamanos NK, Targeting epidermal growth factor receptor in solid tumors: critical evaluation of the biological importance of therapeutic monoclonal antibodies. Curr Med Chem. 2009; 16: 3797–3804.

28. Xu J, Rodriguez D, Petieclere E, Kim JJ, Hangai M, Moon YS, Davis GE and Brooks PC. Proteolytic exposure of a cryptic site within collagen type IV is required for angiogenesis and tumor growth in vivo. J Cell Biol. 2001; 154: 1069–1080.

29. Koshikawa N, Giannelli G, Cirulli V, Miyazaki K and Quaranta V. Role of cell surface metalloprotease MT1-MMP in epithelial cell migration over laminin-5. J Cell Biol. 2000; 48: 615–624.

30. Baciu PC, Suleiman EA, Deryugina EI and Strongin AY. Membrane type-1 matrix metalloproteinase (MT1-MMP) processing of pro-alphav integrin regulates cross-talk between αvβ3 and α2β1 integrins in breast carcinoma cells. Exp Cell Res. 2003; 291: 167–175.

31. Stetler-Stevenson WG. Matrix metalloproteinases in angiogenesis: a moving target for therapeutic intervention. J. Clin. Investig. 1999; 103: 1237–1241.

32. Eliceiri BP, and Cheresh DA. Adhesion events in angiogenesis. Curr. Opin. Cell Biol. 2001; 13: 563–568.

33. Naglich G, Jure-Kunkel M, Gupta E, Fargnoli J, Henderson AJ, Lewin AC, Talbott R, Baxter A, Bird J, Savopoulos R, Wills R, Kramer RA, and Trail PA. Inhibition of angiogenesis and metastasis in two murine models by the matrix metalloproteinase inhibitor. BMS-275291. Cancer Res. 2001; 61: 8480–8485.

34. Mamelak AN, Jacoby DB. Targeted delivery of antitumoral therapy to glioma and other malignancies with synthetic chlorotoxin (TM-601). J. Drug Deliv. 2007; 4: 175-186.

35. Shen S, Khazaeli MB, Gillespie GY, et al. Radiation dosimetry of ^{131}I-chlorotoxin for targeted radiotherapy in glioma-bearing mice. J Neuro Oncol. 2005; 71: 113-119.

36. Soroceanu L, Manning TJ, and Sontheimer H. Modulation of glioma cell migration and invasion using Cl(-) and K(+) ion channel blockers. J. Neurosci. 1999; 19: 5942–5954.

37. McFerrin MB, and Sontheimer, H. A role for ion channels in glioma cell invasion. Neuron Glia Biol. 2006; 2: 39–49.

38. Deshane J, Garner CC, and Sontheimer H. Chlorotoxin inhibits glioma cell invasion via matrix metalloproteinase-2. J. Biol. Chem. 2003; 278: 4135–4144.

39. Lyons SA, O'Neal J, and Sontheimer H. Chlorotoxin, a scorpion-derived peptide, specifically binds to gliomas and tumors of neuroectodermal origin. Glia. 2002; 39: 162–173.

40. Veiseh M, Gabikian P, Bahrami SB, Veiseh O, Zhang M, Hackman RC, Ravanpay A C, Stroud MR, Kusuma Y, Hansen SJ, Kwok D, Munoz NM, Sze RW, Grady WM,

Greenberg NM, Ellenbogen RG, and Olson JM. Tumor paint: a chlorotoxin: Cy5.5 bioconjugate for intraoperative visualization of cancer foci. Cancer Res. 2007; 67: 6882–6888.

41. Lasic DD, Templeton NS. Liposomes in gene therapy. Adv Drug Deliv Rev. 1996; 20: 221–226.
42. Kozubek A, Gubernator J, Przeworska E, Stasiuk M. Liposomal drug delivery, a novel approach: PLARosomes. Acta Biochim Pol. 2000; 47: 639–649.
43. Barenholz Y. Liposome application: problems and prospects. Curr Opin Colloid Interface Sci. 2001; 6: 66–77.
44. Bangham AD, Standish MM, Watkins JC. Diffusion of univalent ions across the lamellae of swollen phospholipids. J Mol Biol. 1965; 13: 238–252.
45. Morgan RA, Anderson WF. Human gene therapy. Annu Rev Biochem. 1993; 62: 191–217.
46. Mortimer I, Tamp P, MacLachlan I, Graham RW, Saravolac EG, Joshi PB. Cationic lipid-mediated transfection of cells in culture requires mitotic activity. Gene Ther. 1999; 6: 403–411.
47. Poste G, Papahadjopoulos D, Vail WJ. Lipid vesicles as carriers for introducing biologically active materials into cells. In: Prescott DM, editor. Methods in Cell Biology. New York (NY): Academic Press. 1976; 8: 33–71.
48. Gregoriadis G, Wills EJ, Swain CP, Tavill AS. Drug-carrier potential of liposomes in cancer chemotherapy. Lancet. 1974; 1: 1313–1316.
49. Kulpa CF, Tinghitella TJ. Encapsulation of polyuridylic acid in phospholipid vesicles. Life Sci. 1976; 19: 1879–1888.

50. Maruyama K, Yuda T, Okamoto T A, Kojima S, Suginaka A, Iwatsuru M. Prolonged circulation time in vivo of large unilamellar liposomes composed of distearoyl phosphatidylcholine and cholesterol containing amphipathic poly (ethylene glycol). Biochim. Biophys. Acta. 1992; 1128: 44–49.

51. Gabizon A, Papahadjopoulos D. Liposome formulation with prolonged circulation time in blood and enhanced uptake by tumors. Proc. Natl. Acad. Sci. USA. 1988; 85: 6949–6953.

52. Vyas SP, Singh A, Sihorkar V. Ligand-receptor-mediated drug delivery: an emerging paradigm in cellular drug targeting, Crit. Rev. Ther. Drug Carrier Syst. 2001; 18: 1–76.

53. Willis M, Forssen E. Ligand-targeted liposomes. Adv. Drug Deliv. Rev. 1998; 29: 249–271.

54. Klibanov AL, Maruyama K, Torchilin VP, Hunag L. 1990. Amphipathic polyethylenglycols effectively prolong the circulation time of liposomes. FEBS Lett. 1990; 268: 235–237.

55. Matsumura Y, Maeda H. 1986. A new concept for macromolecular therapeutics in cancer chemotherapy: mechanism of tumoritropic accumulation of proteins and the antitumor agent smancs. Cancer Res. 1986; 46: 6387–6392.

56. Knauper V, Will H, Lopez-Otin C, Smith B, Atkinson SJ, Stanton H, Hembry, RM, Murphy G. Cellular mechanisms for human procollagenase-3 (MMP-13) activation. Evidence that MT1-MMP (MMP-14) and gelatinase a (MMP-2) are able to generate active enzyme. J. Biol. Chem. 1996; 271: 17124–17131.

57. Noel A, Santavicca M, Stoll I, L'Hoir C, Staub A, Murphy G, Rio MC, Basset P. Identification of structural determinants controlling human and mouse stromelysin-3 proteolytic activities. J. Biol. Chem. 1995; 270: 22866–22872.

58. Ohuchi E, Imai K, Fujii Y, Sato H, Seiki M, Okada Y. Membrane type 1 matrix metalloproteinase digests interstitial collagens and other extracellular matrix macromolecules. J. Biol. Chem. 1997; 272: 2446–2451.

59. Pei D, Majmudar G, Weiss SJ. Hydrolytic inactivation of a breast carcinoma cell-derived serpin by human stromelysin-3. J. Biol. Chem. 1994; 269: 25849–25855.

60. Pei D, Weiss SJ. Transmembrane-deletion mutants of the membrane-type matrix metalloproteinase-1 process progelatinase A and express intrinsic matrix-degrading activity. J. Biol. Chem. 1996; 271: 9135–9140.

61. Sato H, Takino T, Okada Y, Cao J, Shinagawa A, Yamamoto E, Seiki M. A matrix metalloproteinase expressed on the surface of invasive tumour cells. Nature. 1994; 370: 61–65.

62. Strongin, AY, Collier I, Bannikov G, Marmer BL, Grant GA, Goldberg GI. Mechanism of cell surface activation of 72-kDa type IV collagenase. Isolation of the activated form of the membrane metalloprotease. J. Biol. Chem. 1995; 270: 5331–5338.

63. Maekawa R, Maki H,Yoshida H, Hojo K, Tanaka H,Wada T, et al. Correlation of antiangiogenic and antitumor efficacy of N-biphenyl sulfonylphenylalanine hydroxiamic acid

(BPHA), an orally active, selective matrix metalloproteinase inhibitor. Cancer Res. 1999; 59: 1231–1235.

64. Nelson NJ. Inhibitors of angiogenesis enter phase III testing. J. Natl. Cancer Inst. 1998; 90: 960–963.

65. Maeda N, Takeuchi Y, Takada M, Sadzuka Y, Namba Y, Oku N. Anti-neovascular therapy by use of tumor neovasculature-targeted long circulating liposomes. J. Control. Release. 2004; 100: 41–52.

CHAPTER 2

Chlorotoxin-Fc Fusion Inhibits Release of MMP-2 from Pancreatic Cancer Cells

ABSTRACT

Chlorotoxin (CTX) is a 36-amino acid peptide derived from *Leiurus quinquestriatus* (scorpion) venom, which inhibits low-conductance chloride channels in colonic epithelial cells. It has been reported that CTX also binds to matrix metalloproteinase-2 (MMP-2), membrane type-1 MMP, and tissue inhibitor of metalloproteinase-2, as well as CLC-3 chloride ion channels, and other proteins. Pancreatic cancer cells require the activation of MMP-2 during invasion and migration. In this study, the fusion protein was generated by joining the CTX peptide to the amino terminus of the human IgG-Fc domain without a hinge domain, the monomeric form of chlorotoxin (M-CTX-Fc). The resulting fusion protein was then used to target pancreatic cancer cells (PANC-1) in vitro. M-CTX-Fc decreased MMP-2 release into the media of PANC-1 cells in a dose-dependent manner. M-CTX-Fc internalization into PANC-1 cells was observed. When the cells were treated with chlorpromazine (CPZ), the internalization of the fusion protein was reduced, implicating a clathrin-dependent internalization mechanism of M-CTX-Fc in PANC-1 cells. Furthermore, M-CTX-Fc clearly exhibited the inhibition of the migration depending on the concentration, but human IgG, as negative control of Fc, was not affected. The M-CTX-Fc may be an effective instrument for targeting pancreatic cancer.

1. INTRODUCTION

Pancreatic cancer is the fourth most common cause of cancer-related mortality worldwide [1] and is characterized by local invasion, early metastasis, and a strong desmoplastic reaction [2]. For these purpose, molecules that inhibit matrix metalloproteinase (MMP) activity or induce the expression of their natural inhibitors, the tissue inhibitor of metalloproteinases (TIMPs), are potentially interesting [3]. Many MMP inhibitors have been developed for human clinical trials, but effective candidates have not yet been identified [4, 5]. In vitro studies have demonstrated that the proteolytic degradation of extracellular matrix (ECM) components is a major step in tumor invasion [6]. Among the enzymes involved in ECM degradation, the MMP family that contains at least 25 members of metzincin endopeptidases is the most studied. These enzymes are able to degrade ECM components [7-9]. MMPs are further divided into two subgroups based on whether the enzyme is either secreted or expressed on the cell surface in a membrane-tethered form; soluble MMPs and membrane type MMPs (MT-MMPs) [10]. Soluble MMPs are secreted from cells into the extracellular milieu and can diffuse to distal sites. Therefore, it is believed that this type of MMP is useful for the degradation of ECM in a wider area [11, 12]. Because collagen IV is one of the major components of the basement membrane, MMP-2, a 72-kDa type IV collagenase, is believed to be of special significance during tumor invasion [2, 13].

MMP-2 is secreted as a proenzyme (proMMP-2) and located on the cell surface of tumor cells and requires activation to exert its catalytic activation [2, 14]. MT1-MMP is expressed as a 63-kDa protein on the surface of tumor cells and acts as a cell-surface

receptor and activator of proMMP-2 [15]. MT1-MMP on the cell surface is replenished by clathrin-dependent internalization, and its concentration is stabilized by TIMP-2 [16, 17].

Chlorotoxin (CTX) is a 36-amino acid peptide which contains four disulfide bridges and is derived from Leiurus quinquestriatus (scorpion) venom. Early studies demonstrated that CTX can inhibit a potentially glioma-specific chloride ion channel [18]. CTX is believed to bind a lipid raft-anchored complex that contains MMP-2 [19], membrane type-1 MMP, tissue inhibitor of metallopreotease-2 [20], and other proteins [21]. In addition to glioma cells, CTX has been shown to specifically bind to other tumors of neuroectodermal origin [22]. It was recently found that CTX not only binds a wide range of tumor cell types but is also internalized by proliferating human vascular endothelial cells [23]. More recently, the in vitro and in vivo tumor-targeting properties of CTX have been shown to retain following conjugation to a fluorescent dye [24], nanoparticles [25-27], and polymers [28].

We have previously reported CTX-dependent inhibition of proliferation and motility in glioblastoma cells using a targeted bionanocapsule displaying the monomeric fusion protein of chlorotoxin (M-CTX-Fc). Moreover, M-CTX-Fc had a more efficient inhibitory effect on migration than CTX. We observed cellular uptake of the bionanocapsules, indicating M-CTX-Fc is an effective vehicle as a drug delivery system.

MMPs are overexpressed in a variety of malignant tumors, including brain, pancreas, prostate, ovarian, bladder, and lung, and they act as ECM-remodeling enzymes; therefore, targeting of these molecules in cancer therapy is a promising approach to suppress their malignancy. The PANC-1, the human cell line derived from pancreatic carcinoma, is over-

expressing MMP-2, MT1-MMP, and MT2-MMP [2]. Thus, the aim of this study was to identify the inhibitory mechanism of M-CTX-Fc on MMP-2 in PANC-1.

2. MATERIALS AND METHODS

2.1. Cell Culture

The human cell line derived from pancreatic carcinoma, PANC-1 (RCB2095), and the glioblastoma, A172 (RCB2530), were provided by the National BioResource Project of MEXT, Japan. Human breast carcinoma derived cell line SKBR-3 was obtained from ATCC (Manassas, VA). The cells were grown and subcultured in RPMI medium (Sigma-Aldrich, St Louis, MO, USA) supplemented with 10% fetal bovine serum (FBS, PAA Laboratories, Pasching, Austria) in the presence of 100 IU/mL penicillin and 100 μg/mL streptomycin (Nacalai Tesque, Kyoto, Japan). The cells were maintained at 37°C in a humidified incubator with 95% air and 5% CO2.

2.2. Expression and Purification of M-CTX-Fc

The preparation of M-CTX-Fc was performed as previously described [29]. Escherichia coli BL21 (DE3) pLysS (Novagen) was transformed with expression vector for M-CTX-Fc. Transformant was grown in 1 L of LB medium containing 50 μg/mL kanamycin and 10 μg/mL chloramphenicol at 37°C. Protein expression was induced by 0.4 mM isopropyl 1-thio-β-D-galactopyranoside. After expression induction, the transformant was cultured at 25°C for 16 h, and the bacteria were harvested. Cell pellets were thawed and homogenized in 20 mL of lysis buffer containing 10 mMTris-HCl (pH 8.0), 10 mM EDTA, 0.2 M NaCl, and 10% sucrose. The inclusion bodies were collected by centrifugation at 12,000 ×g for 20 min. The inclusion bodies were washed three times with 0.5% Triton X-100. The insoluble fraction was resolved in 4 mL of 6 M guanidinium HCl

containing 0.1 M Tris-HCl (pH 8.5). The solution was degassed by aspiration while purging the air with nitrogen gas and supplemented with 50 μL of β-mercaptoethanol. After 1 h incubation at 37°C in a shaking water bath, the mixture was dispersed into a 20-fold volume of refolding buffer containing 10 mM Tris-HCl (pH 8.5), 0.1 M NaCl, and 0.5 mM oxidized glutathione. Refolding was conducted by incubation at 4°C for 18 h. The pH was then adjusted to 7.0 using acetic acid. Insoluble materials were removed by centrifugation at 12,000×g for 20 min. The solution containing refolded protein was applied to a cobalt resin column (TALON super flow metal affinity resin, Clontech, Mountain View, CA, USA), after equilibrating with equilibration buffer containing 50 mM phosphate buffer (pH 7.0) and 300 mM NaCl. The column was then washed with equilibration buffer containing 20 mM imidazole and 0.1% Triton X-100. M-CTX-Fc was eluted with elution buffer containing 50 mM phosphate buffer (pH 7.0), 300 mM imidazole, and 300 mM NaCl. The eluted solution was dialyzed three times against phosphate-buffered saline (Dulbecco's formula, hereafter PBS) for 2 h each time. The purity of M-CTX-Fc in the final preparations was assessed by SDS-PAGE, Coomassie Brilliant Blue (CBB) staining, and western blotting.

2.3. Preparation of the Conditioned Media for Zymography and western blot

PANC-1 cells were seeded at a density of 1.0×10^5 cells per 35-mm dish in RPMI medium supplemented with 10% FBS. After 20 h of culture, the cells were washed with serum-free medium and incubated for an additional 24 h in the same serum-free medium with and without 12, 60, and 300 nM human IgG (Sigma), CTX (AnaSpec Inc. Fremont), and M-CTX-Fc, respectively. The conditioned media (CM) was collected and centrifuged

to remove insoluble materials and then stored at −80°C until used in zymography and western blotting.

2.4. Gelatin Zymography

MMP-2 gelatinolytic activity was determined in the CM of PANC-1 cells. Fifteen-microliter aliquots of CM were subjected to SDS-PAGE (10%) in the presence of 0.05% gelatin. The samples were not boiled prior to electrophoresis. After electrophoresis, the gels were washed twice in 2.5% Triton X-100 for 30 min and once in 50 mM of Tris-HCl (pH 7.4) for 15 min. The gels were then incubated for 16–20 h at 37°C in buffer A, which contained 30 mM Tris-HCl (pH 7.4), 5 mM CaCl2, 0.5 μM ZnCl2, 0.2 M NaCl, and 0.02% NaN3. After incubation, the gels were stained with Coomassie brilliant blue in 50% methanol and 10% acetic acid and destained in 10% methanol and 10% acetic acid.

2.5. Quantitative real-time PCR (qRT-PCR)

PANC-1 cells were untreated or treated with 300 nM M-CTX-Fc for 6 and 24 h. Total RNA was isolated from cells using an RNeasy Minikit (Qiagen). Two micrograms of the total RNA was transcribed with superscript II (Invitrogen) in accordance with the manufacture’s protocol. The primer sequences of MMP-2 were: forward primer 5′-TTTCCATTCCGCTTCCAGGGCACAT-3′ and reverse primer 5′-TCGCACACCACATCTTTCCGTCACT-3′. qRT-PCR was performed with SYBR Green Real time Master Mix (Toyobo, Japan) in triplicate containing 5 ng of cDNA along with 400 nM primers using a LightCycler system (TM Roche). The thermal cycling condition

was as follows: 95°C for 5 min followed by 45 cycles of 95°C for 10 s, 57°C for 10 s, and 72°C for 12 s.

2.6. Biotinylation Assay for the Internalization of M-CTX-Fc

Biotinylation was performed as described previously [30]. PANC-1 cells were plated in a 60-mm tissue culture dish in complete medium. At 90% confluency, the cells were washed twice in Hank's balanced salt solution (HBSS) for 10 min at 4°C. Sulfo-NHS-SS-Biotin (Thermo Scientific) dissolved in HBSS at a concentration of 0.5 mg/mL, was added to the cells at 4°C with mild shaking for 20 min, and this reaction was repeated twice. The cells were washed with HEPES buffered RPMI supplemented with 1% BSA and 2 mM glutamine (RPMI-BSA) for 10 min at 4°C. Control cells were incubated with RPMI-BSA for 1 h at 37°C. The cells were then incubated with either 300 nM M-CTX-Fc or human IgG in RPMI-BSA for 1 h at 4°C or 37°C. The treatment was stopped by placing the dishes back on ice and rinsing the cells twice with HBSS. The biotin on the cell surface was cleaved by incubation of the cells in a reducing solution consisting of 20 mM DTT, 50 mM Tris-HCl (pH 8.7), 100 mM NaCl, and 2.5 mM CaCl2 for 20 min at 4°C and was repeated twice. The cells were washed thrice with HBSS, scraped off with lysis buffer consisting of 1% Triton X-100, 50 mM Tris-HCl (pH 7.4), 150 mM NaCl, 5 mM EDTA, 1 mM PMSF, and protease inhibitor cocktail (Sigma-Aldrich) and incubated for 20 min at 4°C. The lysates were collected and sonicated twice, and cell extracts were clarified by centrifugation for 5 min at 4°C. Protein concentrations in the extracts were determined by a BCA assay (Pierce Chemical). Twenty microliters of avidin agarose (Sigma-Aldrich) were added to the extracts, which were incubated overnight at 4°C. After centrifugation for 30 s at 4°C, the

agarose was washed thrice in lysis buffer, suspended in Laemmli buffer with β-mercaptoethanol, heated for 5 min at 95°C, and finally processed for western blotting. Transferrin receptor internalization was used as a control for immunoprecipitation experiments.

2.7. Western Blotting and Image Analysis

One hundred fifty microliters of the CMs were concentrated 10-fold by the methanol/chloroform/water method. The concentrated CM samples were resolved in Laemmli-buffer supplemented with β-mercaptoethanol and subjected to SDS-PAGE and western blotting. Proteins resolved on SDS-PAGE were transferred to a polyvinylidene difluoride (PVDF) membrane (Millipore, Billerica, MA, USA). The membrane was blocked with 10% skim milk in 10 mM Tris-HCl (pH 7.4), 150 mM NaCl containing 0.1% Tween-20 (TBST). To detect MMP-2, the blots were probed with anti-MMP-2 rabbit antibody (abcam) and anti-rabbit (IgG) goat antibody conjugated with HRP (Cell signaling technology, Beverly, MA, USA). To assay biotinylation, the blots were probed with anti-human IgG mouse monoclonal antibody conjugated with HRP (Life Technologies, Carlsbad, CA, USA) diluted to 1:1000 in TBST containing 10% skim milk, anti-transferrin receptor mouse monoclonal antibody diluted 1:1000 (Invitrogen), followed by anti-mouse IgG horse antibody conjugated with HRP diluted 1:2000 (Cell Signaling Technology, Beverly, MA, USA). The HRP signal was developed using a Western Lightning Plus-ECL chemiluminescence reagent (PerkinElmer, Waltham, MA, USA), and the intensities of the bands were visualized using a Light-Capture II cooled CCD camera system (ATTO, Tokyo,

Japan). Quantitative assessments of the relative intensity of the blots were analyzed using Image J.

2.8. Confocal Microscopic Observation

For confocal microscopic observation, PANC-1 cells were grown on 18-mm cover slips (Iwaki, Tokyo, Japan) in 12-well plates. The cells were incubated with 300 nM M-CTX-Fc [30] in PBS containing 1% BSA for 30 min at 4°C or 37°C. The cells were washed twice with PBS to evaluate specific binding to cell surfaces. The cells were fixed with 4% paraformaldehyde in PBS, permeabilized with 0.2% Triton X-100, and blocked with a blocking solution containing 10% FBS or 1% BSA in PBS. The cells were washed with PBS and incubated with anti-early endosome antigen-1 (EEA-1) antibody (Cell Signaling Technology, Beverly, MA, USA) for 1 h at 25°C followed by Alexa 555-labeled anti-rabbit IgG (Molecular Probes Inc., Eugene, OR, USA) for 30 min at 25°C. The cells were washed with PBS and incubated with FITC-labeled anti-human IgG-Fc antibody (Sigma-Aldrich) for 1 h at 25°C. After further washes, the nuclei were stained with DAPI (Vector Laboratories Inc., Burlingame, CA, USA), and the cells were visualized using a confocal microscope (IX81; Olympus) with Fluoview FV-1000 (Olympus).

2.9. Cell Proliferation Assay

The effect on cell proliferation in PANC-1 cells by M-CTX-Fc was evaluated by cell count. PANC-1 cells were seeded onto 12-well plates at a density of 3×10^4 or 1×10^5 cells/well, and cultured in RPMI medium supplemented with 10% FBS. After 20 h of culture, M-CTX-Fc in a range of 0–300 nM were added in triplicate, and the cells were

further cultured for 24 h or 48 h. The cells were then trypsinized and counted with TC10 automated cell counter (Bio-Rad, Hercules, CA, USA).

The inhibition of cell growth by human IgG, CTX, and M-CTX-Fc was evaluated using a 3-(4, 5-dimethylthiazol-2-yl)-2, 5-diphenyltetrazolium bromide (MTT) cleavage assay. The cells were seeded at a density of 5×10^3 cells/well in 96-well plates in RPMI medium supplemented with PANC-1 and 10% FBS. After 20 h of culture, human IgG, CTX, and M-CTX-Fc in a range of 0–300 nM were added in triplicate, and the cells were further cultured for 48 h. The cells were then exposed to 5 mg/mL MTT in PBS at a final concentration of 1 mg/mL in culture for 5 h. Formazan crystals formed during the incubation period were dissolved overnight at 37°C by adding 10% SDS containing 20 mM HCl. The absorbance was measured at 570 nm. To assess the viability of cells treated with CTX and M-CTX-Fc after 48 h incubation with different concentrations of CTX and M-CTX-Fc, the wells were washed twice with RPMI medium supplemented with 10% FBS. The cells were further incubated for 48 h in RPMI medium supplemented with 10% FBS. The viable cells were evaluated using the MTT cleavage assay, as described above.

2.10. Cell Migration Assay

The migration of PANC-1 cells was assayed in 24-well plates with 8-μm pore cell culture inserts (BD, Franklin Lakes, NJ, USA). Five hundred microliters of RPMI medium supplemented with 10% FBS were added to each well, and 3×10^4 cells were seeded into each insert. The cells were incubated with human IgG, CTX, and M-CTX-Fc, in a range of 0–300 nM in RPMI medium supplemented with 1% BSA at 37°C. After 48 h of culture, the insert chambers were removed and adherent cells on the bottom of each well were counted

under microscope. The number of migrated cells was normalized to the number of adherent cells in the absence of human IgG, CTX, and M-CTX-Fc.

2.11. Statistical Analysis

The Data is expressed as the mean ± SE. The statistical significance of differences between means was determined using Student's t test. Differences were statistically significant at $P < 0.05$.

3. RESULTS

3.1. Preparation of M-CTX-Fc

The His-tagged CTX-Fc fusion protein was designed as a CTX peptide fused with to the amino terminus of the human IgG-Fc domain without a hinge domain. The CTX-Fcs expressed in E. coli were observed as monomers of approximately 30 KDa under the reducing condition, which was confirmed by western blotting (Fig. 1)

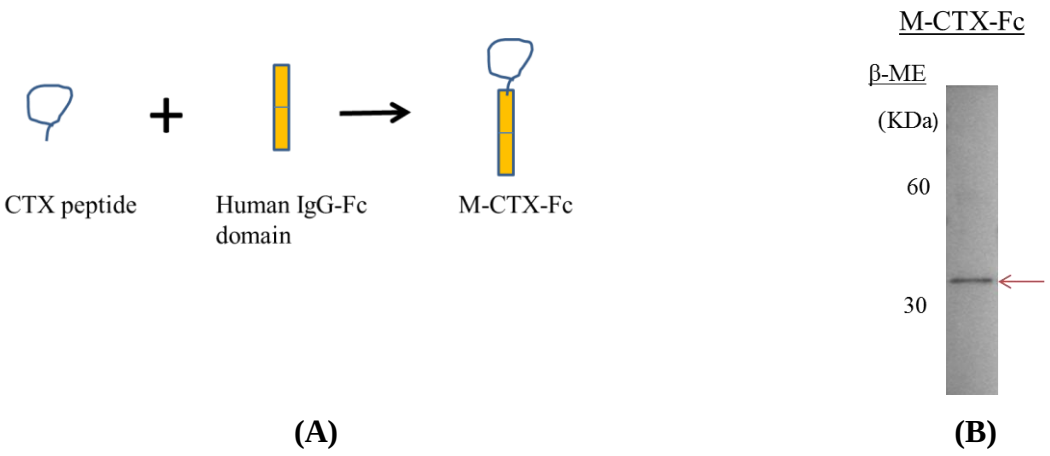

Figure 1: *Preparation of M-CTX-Fc.* (a) Schematic diagram of monomeric CTX-Fc. (b) Reduced form of M-CTX-Fc. M-CTX-Fc was subjected to SDS-PAGE and western blotting. Anti-human-IgG-Fc antibody reacted with the purified M-CTX-Fc without significant degradation. Arrow indicates the purified protein. ß-ME: beta-membrane; WB: western blotting.

3.2. PANC-1 cells express MMP-2

The 72-KDa protein reacted with anti-MMP2 antibody corresponding to proMMP-2 was observed in PANC-1 and glioma cells (A172) but not in SKBR-3 cells (used as a no/low-expressing control) [31] (Figure 2A). A172, in which the expression of MMP-2 is well known, was used as a positive control. Also, the expression of MMP-2 was confirmed by immunocytochemistry(Figure 2C). Because PANC-1 cells were confirmed to express the MMP-2 protein, we studied the effect of M-CTX-Fc on PANC-1 cells hereafter.

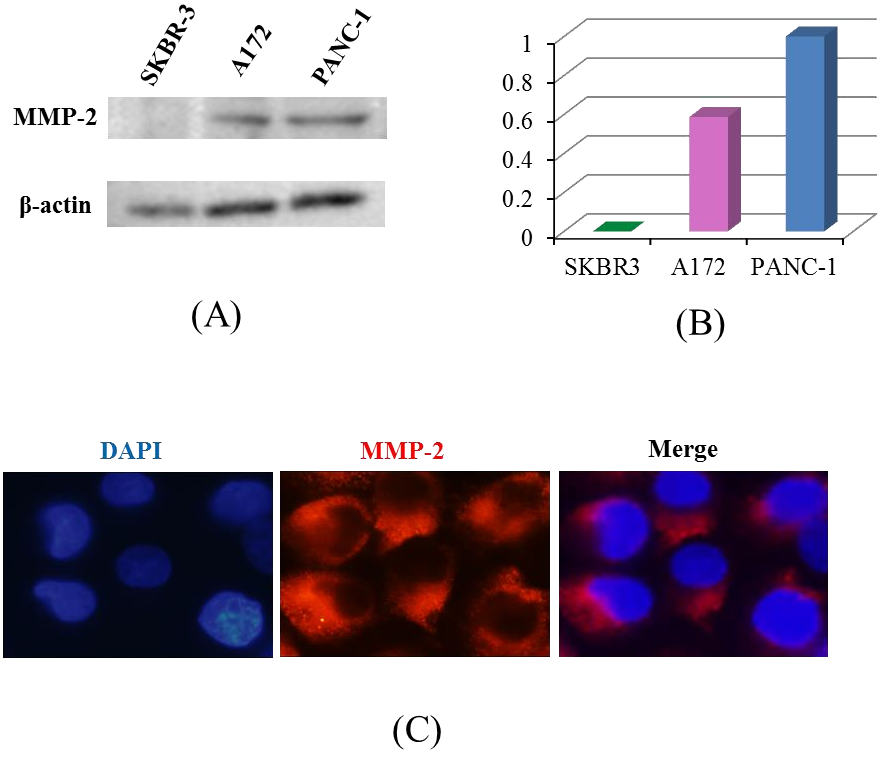

Figure 2: *Expression of matrix metalloproteinase-2 (MMP-2) in PANC-1.* **(A)** The protein extracted from SKBR-3 (as a negative control), A172 (as a positive control), and PANC-1 were immunoblotted and detected using anti-MMP2 antibody. β-actin was used as loading

control. **(B)** The intensity of each band was densitometrically analyzed by Image J and plotted. **(C)** Immunostaining for MMP-2 in PANC-1 cells.

3.3. Effect of M-CTX-Fc on the Secretion of MMP-2

To examine the changes in activity and the expression of MMP-2 in the presence of human IgG (negative control), CTX (positive control), and M-CTX-Fc, gelatinase activity in the CM from PANC-1 cells was analyzed by gelatin zymography. Cells were treated with incremental concentrations of human IgG, CTX, and M-CTX-Fc in a range of 0–300 nM for 1, 3, 6, 12, and 24 h. The effect of human IgG, CTX, and M-CTX-Fc on MMP-2 zymogen in the CM was determined. M-CTX-Fc caused dose-dependent reduction in the amount of zymogen (72-KDa MMP-2 proenzyme) in the CM of PANC-1 cells at 1, 3, 6, 12, and 24 h (Figure 3A). In contrast, amount of MMP-2 proenzyme was not significantly affected by human IgG and CTX (Figure 3A). The M-CTX-Fc in a range of 0-300 nM did not inhibit the cell proliferation (Figure 3B). The result indicated that the inhibition of MMP-2 secretion was not due to M-CTX-Fc cytotoxicity.

The decrease in the amount of MMP-2 was confirmed by western blotting. PANC-1 cells were treated with 12, 60, and 300 nM of human IgG, CTX, and M-CTX-Fc, respectively, for 24 h, and then the CMs were concentrated. The effect of human IgG, CTX, and M-CTX-Fc on MMP-2 protein secretion levels in the CM was determined by western blotting analysis using antibodies recognizing the MMP-2. M-CTX-Fc decreased the levels in the CM of PANC-1 cells in a dose-dependent manner in the range of 0–300 nM. At a concentration of 300 nM M-CTX-Fc, 79% of MMP-2 release was suppressed (Figure 3C).

In contrast, human IgG and CTX treatment did not cause noticeable variation of MMP-2 levels (Figure 3C).

To determine whether the decrease in the MMP-2 protein expression correlates with MMP-2 gene expression, we performed qRT-PCR that showed the MMP-2 gene expression was not significantly affected by M-CTX-Fc in PANC-1 cells (Figure 3D). The decrease of the amount of MMP-2 proenzyme secreted into CM may be caused by the decrease in the release of MMP-2 into the CM.

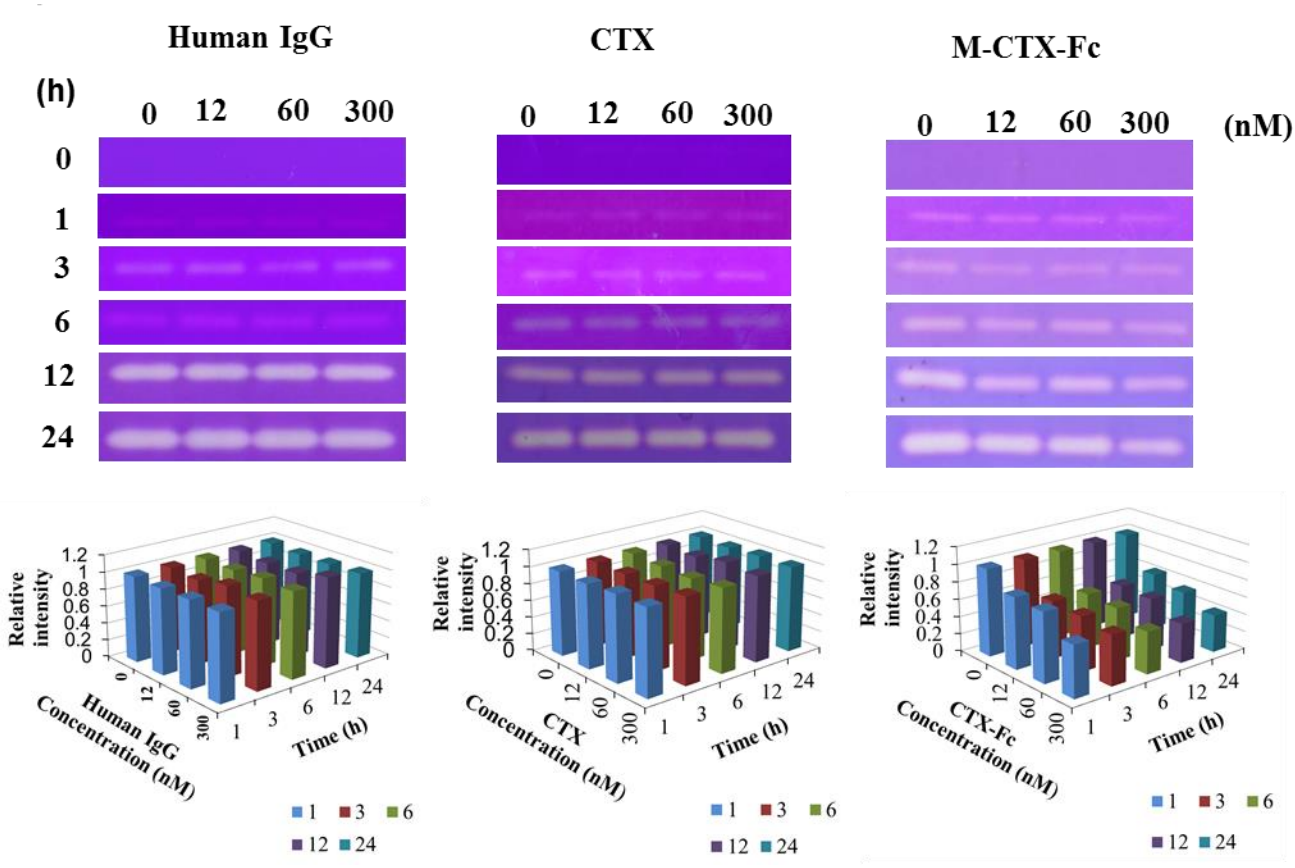

(A)

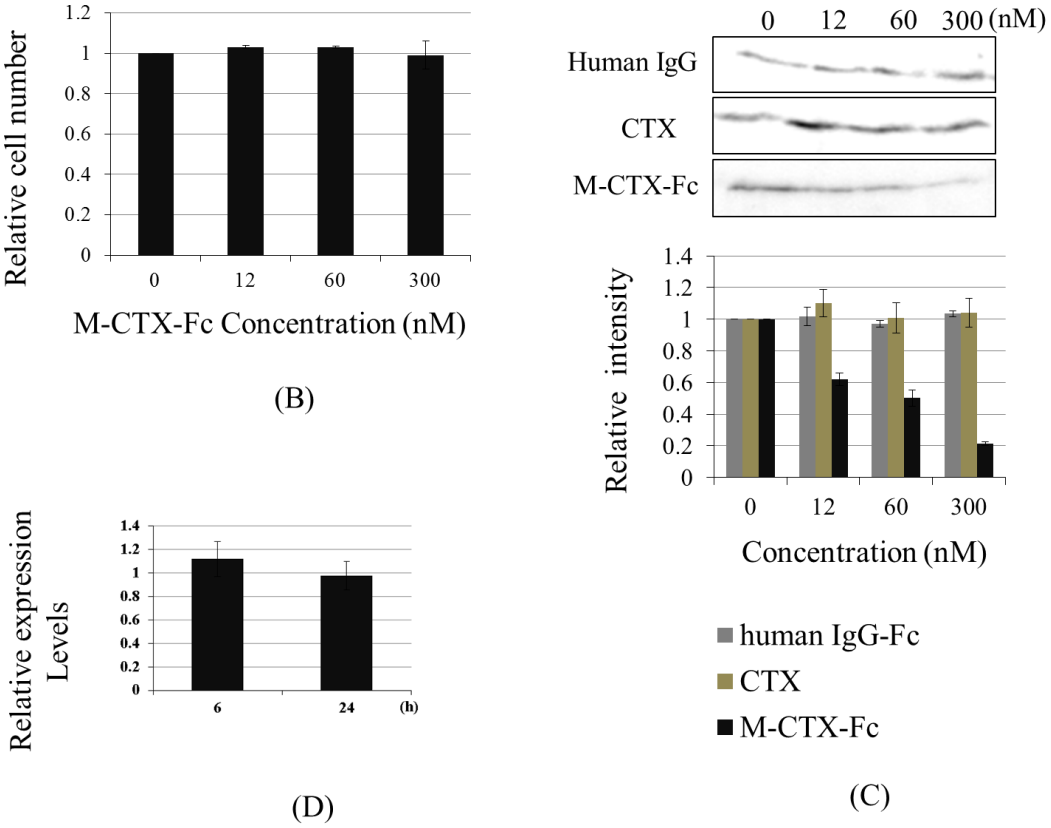

Figure 3: (A) Gelatinase activities of conditioned media (CM) from cultured PANC-1 cells. Cells were treated with 0, 12, 60, and 300 nM human IgG, chlorotoxin (CTX), and M-CTX-Fc at 1, 3, 6, 12, and 24 h. Each 15 μL of the CM were subjected to gelatin zymography. **(B)** PANC-1 cells were seeded onto 12-well plates at a density of 1×10^5 cells/well and cultured. After 20 h of culture, M-CTX-Fc at a range of 0–300 nM was added to each well for 24 h, and then the cells were trypsinized and counted. **(C)** M-CTX-Fc decreased MMP-2 release in PANC-1 cells. PANC-1 cells were treated with incremental concentrations of human IgG, CTX, and M-CTX-Fc for 24 h. The CM were collected and concentrated. The protein in the CM was separated using 10% SDS-PAGE, transferred to a PVDF membrane, and probed with monoclonal MMP-2 antibody. **(D)** qRT-PCR analysis of MMP-2 expression in the absence and presence of M-CTX-Fc. qRT-PCR analysis was performed using primers for MMP-2. Primers specific for GAPDH were used as an internal control. PCR products were separated using 2% TAE agarose gel electrophoresis.

3.4. Intracellular Localization of M-CTX-Fc in PANC-1 Cells

Because of the high expression levels of MMP-2, we evaluated the binding capability of M-CTX-Fc on the surface of PANC-1 pancreatic cells. When the cells were incubated with M-CTX-Fc at 4°C, the fluorescence from FITC-labeled anti-human IgG indicated localization of the fused proteins on the plasma membrane. However, when the cells were incubated at 37°C, the fluorescence indicated that M-CTX-Fc was localized intracellularly in PANC-1 cells (Figure 4).

Because cells adopt divergent pathways for endocytosis, the key pathways are divided into clathrin-dependent and clathrin-independent mechanisms [32]. The clathrin-independent pathway are further classified into caveolar and GPI-anchored early endocytic compartment (GEEC) pathways [32, 33].

The mechanism of M-CTX-Fc uptake was assessed in PANC-1 cells using endocytotic pathway inhibitors. PANC-1 cells were treated with M-CTX-Fc in the presence or absence of inhibitor for clathrin and the internalization was assessed. When the cells were treated with 100 nM CPZ, an amphiphilic drug, which inhibits the clathrin mediated pathway [30], the internalization of the M-CTX-Fc was reduced (Figure 4).

Most of the cargos irrespective of their route merges with Rab5 and early endosome antigen-1 (EEA-1) enriched in early endosomes, which is further sorted into various intracellular destinations [34]. We thus analyzed the recruitment of M-CTX-Fc into early endosomes using an early endosomal marker EEA1 after M-CTX-Fc stimulation in PANC-1 cells at 4°C and 37°C in the presence and absence of CPZ. Localization in endosomes was not observed in cells after 300 nM M-CTX-Fc treatment for 30 min at 4°C. However Co-localization of M-CTX-Fc with EEA1 was observed beneath the cell membrane of cells

after M-CTX-Fc treatment for 30 min at 37°C which was reduced in the presence of CPZ (Figure 4).

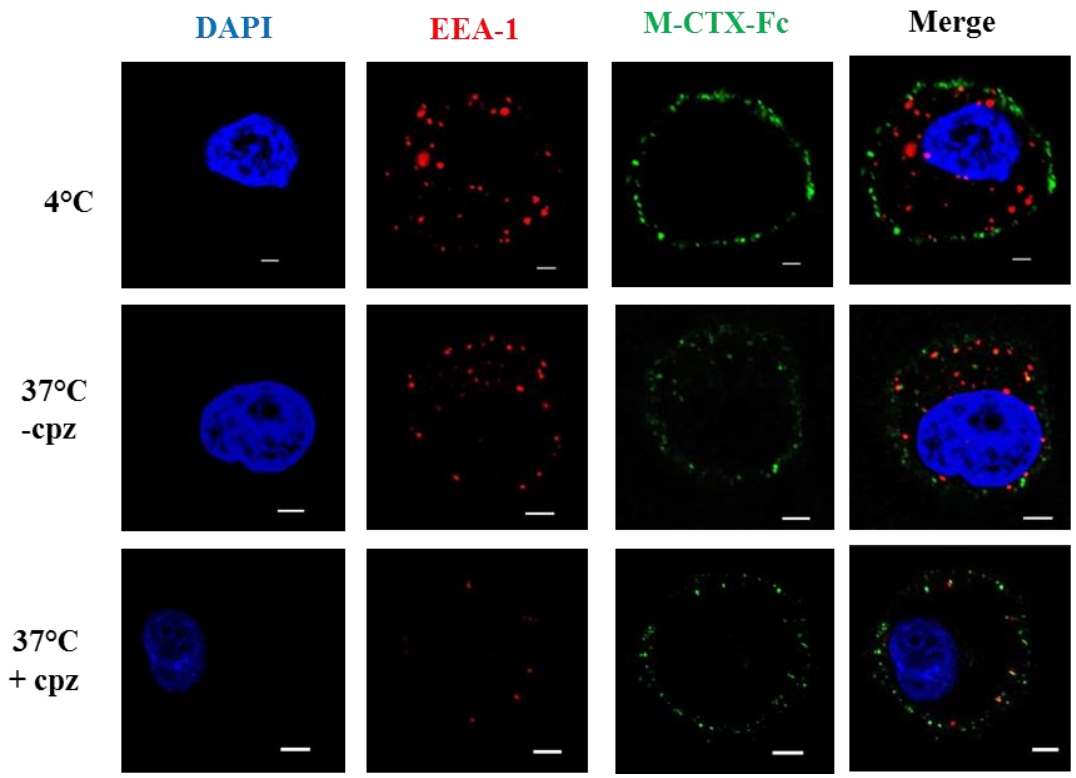

Figure 4: *Evaluation of M-CTX-Fc internalized by PANC-1 cells.* PANC-1 cells were treated with M-CTX-Fc at 37°C and 4°C and stained with FITC-labeled anti-human IgG antibody and with anti-EEA1 antibody followed by a secondary antibody against Alexa flour 555 labeled-Rabbit IgG.

3.5. Internalization of M-CTX-Fc

To determine the amount of internalized M-CTX-Fc that was colocalized with EEA1, biotinylation assay was assessed. Surface biotinylated cells were treated with 300 nM M-

CTX-Fc and human IgG at 37°C for 1 h. The proteins on cell surface were removed by reduction buffer and washing, then only internalized biotinylate proteins were being assessed. Cell lysates were pull-downed with avidin agarose and blotted against anti-human IgG (Fc-domain specific) antibody conjugated with HRP to analyze the intennalized M-CTX-Fc in PANC-1 cells. As for the control, the biotinylated cells were exposed by M-CTX-Fc at 4°C for 1 h. Internalization of the transferrin receptor was also monitored as an endocytosis control.

When the biotinylated cells were treated with 300 nM M-CTX-Fc, the internalization of M-CTX-Fc was increased relative to untreated cells at 37°C (Figure 5). The incubation of cells at 37°C facilitated the intracellular localization of M-CTX-Fc, indicating that the temperature-dependent internalization was attributable to a membrane-dependent mechanism. In contrast, the human IgG produced no internalization at 37°C, indicating specific binding of the CTX moiety to PANC-1 cell surfaces. Without biotinylation, cells incubated with M-CTX-Fc at 37°C produced no signals on western blotting, indicating that the results of immunoprecipitation were detected by biotin-labeling specific reaction (Figure 5).

When the cells were treated with 300 nM of M-CTX-Fc and 100 nM CPZ, the internalization of M-CTX-Fc was reduced. M-CTX-Fc is believed to be internalizing into PANC-1 cells through a clathrin-mediated mechanism.

3.6. Effect of M-CTX-Fc on the Migration of PANC-1 Cells

The effect of human IgG, CTX, and M-CTX-Fc on the migration of PANC-1 cells was assessed (Figure 6A). Although M-CTX-Fc and CTX at a concentration of 300 nM

significantly inhibited the cellular migration, M-CTX-Fc inhibition was clearly concentration-dependent. The maximal inhibition obtained with M-CTX-Fc was 70% compared with untreated control cells. The results showed that M-CTX-Fc had a more efficient inhibitory effect than CTX, which was not observed with human IgG at the same concentration. The M-CTX-Fc in a range of 0-300 nM did not inhibit the cell proliferation (figure 6B). The result indicated that the inhibition of cell migration was not due to cell proliferation.

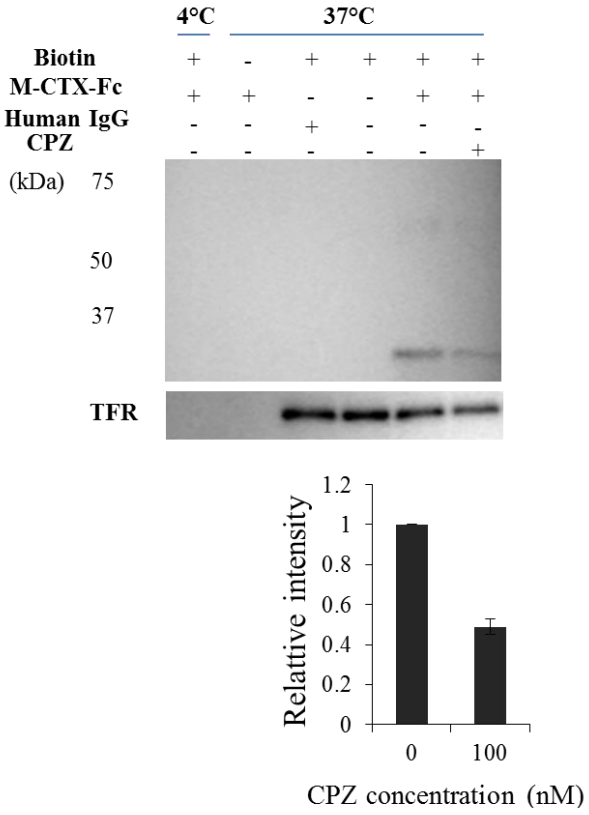

Figure 5: *Evaluation of M-CTX-Fc internalized by PANC-1 cells.* Cell surface receptors were reversibly biotinylated with NHS-SS-Biotin and were incubated with M-CTX-Fc for 1 h. Lane 1: biotinylated cells treated with M-CTX-Fc at 4°C; Lane 2: nonbiotinylated cells treated with M-CTX-Fc at 37°C; Lane 3: biotinylated cells treated with human IgG at 37°C; Lane 4: biotinylated cells left untreated at 37°C for 1 h; Lane 5 and 6: biotinylated cells with M-CTX-Fc at 37°C in the absence and presence of 100 nM CPZ. After treatment, cells were lysed, immunopreciptated with avidin agarose, and subjected to western blot to detect M-CTX-Fc with antihuman IgG antibody. Transferrin was monitored simultaneously as the control for internalization. The intensity of M-CTX-Fc was densitometrically analyzed by ImageJ and plotted to evaluate internalization.

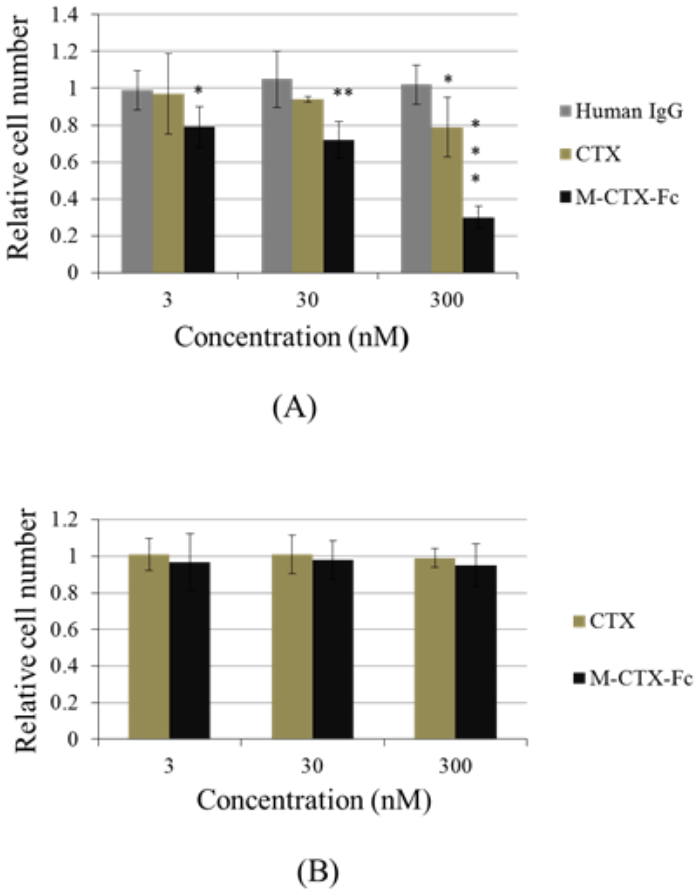

Figure 6: *Cell migration assay.* **(A)** The effect of human IgG, CTX, and M-CTX-Fc on the migration of PANC-1 cells was assessed using a PET track-etched membrane culture insert (pore size, 8.0 μm). 3×10^4 Cells were incubated with human IgG, CTX, and M-CTX-Fc in the range of 0–300 nM. Translocated cell numbers were normalized against those in the absence of human IgG, CTX, and M-CTX-Fc. The results are shown as mean ± SD from three independent experiments. (* $P < 0.1$, ** $P < 0.05$, *** $P < 0.01$). **(B)** PANC-1 cells were seeded onto 12-well plates at a density of 3 × 104 cells/well and cultured. After 20 h of culture, M-CTX-Fc at a range of 0–300 nM was added to each well for 48 h, and then the cells were trypsinized and counted.

3.7. Effect of M-CTX-Fc on the proliferation of PANC-1 Cells

We then evaluated the effects of human IgG, CTX, and M-CTX-Fc on the proliferation and viability of PANC-1 cells. M-CTX-Fc strongly suppressed the cell viability compared with CTX (Figure 7A). The IC_{50} was estimated at approximately 200 nM. After treatment with 300 nM CTX and M-CTX-Fc for 48 h, the growth of cells was resumed in the next 48 h when the medium was replaced with a medium without CTX and M-CTX-Fc (figure 7B).

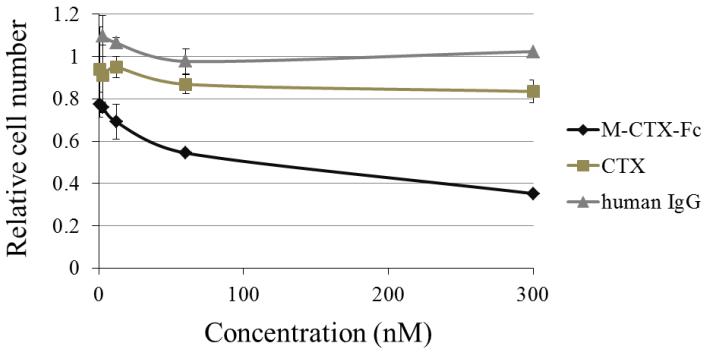

(A)

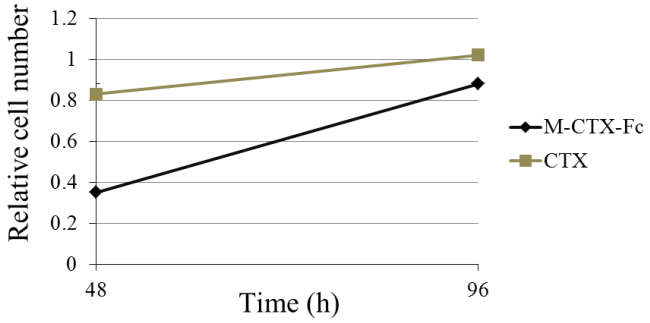

(B)

Figure 7: *Proliferation inhibition activity.* **(A)** Five thousand cells were grown in the presence of CTX and M-CTX-Fc for 48 h. **(B)** The viable cells at 48 h were kept cultured without CTX and M-CTX-Fc up to 96 h. Cell numbers in each well were assessed by a 3-(4,5-dimethylthiazol-2-yl)-2,5-diphenyltetrazolium bromide (MTT) assay. The absorbance at 570 nm corresponding to initial number of cells was defined as 1

4. DISCUSSION AND CONCLUSION

CTX is a 36-amino acid peptide that belongs to a large family of insect toxins. Several recent studies have suggested that CTX is a highly specific ligand for malignant human gliomas and shows no significant binding to normal brain tissue [21]. CTX has been shown to bind to a 68–72-kDa membrane protein in glioma cells, where it causes inhibition of transmembrane Cl− fluxes, presumably by inhibiting Cl− channels. For use as ligands, we designed a fusion protein between CTX and the human IgG-Fc domain, which exists as a 30-kDa monomer (figure 1).

Matrix metalloproteinases (MMPs), zinc endopeptidases, are capable of proteolysis of numerous ECM components. Over 25 members of this family have been identified to date. MMP-2, -3, -7, -9, -11, and -14 have been evaluated in pancreatic cancer cells [35-37]. The mechanism of activation and regulation of MMP-2 is tightly regulated by several other proteins that form a macromolecular complex specifically involving interactions with membrane-associated MT1-MMP (MMP-14) and $\alpha_v\beta_3$ integrin, matrix proteins, and its endogenous inhibitor, TIMP-2 [38, 39]. MT1-MMP, a membrane-type MMP activates MMP-2, and $\alpha_v\beta_3$ integrin promotes the maturation and release of MMP-2 [38, 39]. MMP-2 is secreted from the cell in the proform, which is then extracellularly activated to a 62 kDa mature protease at the cell surface by the membrane-bound MT1-MMP and TIMP-2 [40, 41]. In the present study, we demonstrated MMP-2 expression in PANC-1 cells (Figure 2).

We also evaluated the effect of M-CTX-Fc on MMP-2 proteolytic activity by gelatin zymography. The exposure of M-CTX-Fc decreased the amount of MMP-2 zymogen in a dose-dependent manner (Figure 3A). We detected the amount of MMP-2 in cultured

medium by western blotting analysis. M-CTX-Fc was decreased the levels of MMP-2 presented in the CM of PANC-1 cells in a dose dependent manner (Figure 3C). MMP-2 a key mediator of ECM degradation and cell migration appears to be a target of M-CTX-Fc. Sonthemier et al. identified MMP-2, the membrane type metalloprotease-1 macromolecular complex, and the CLC-3 chloride ion channel as targets for CTX on the surface of human glioma cells [42, 20]. In subsequent studies, Olson et al. also demonstrated that MMP-2 facilitates the binding of CTX to MCF-7 breast cancer cells [24]. However, these studies were unable to demonstrate a direct interaction between CTX-Cy5.5 and recombinant MMP-2, suggesting that the molecular target for CTX is yet unknown [24]. Although we could not confirm the binding between M-CTX-Fc and MMP-2, and MT1-MMP, this is consistent with other research [24]. The exact molecular mechanisms for the decrease of MMP-2 levels into the cell media are currently under investigation.

MT1-MMP is able to internalize into the intracellular space, and like other membrane-binding molecules it is regulated by endocytosis because of the functional role of internalization in the cytoplasmic tail [43]. The regulation of the activity and internalization of MT1-MMP are associated with integrin on the surface of endothelial cells [44]. Endocytosis and accumulation of MT1-MMP are mediated by the clathrin-dependent endocytic pathway [43]. M-CTX-Fc was localized to the intracellular space at 37°C (Figure 4) and was reduced by 100 nM CPZ. The internalization of M-CTX-Fc was also shown to be temperature-dependent (Figure 5). The human IgG produced no internalization at 37°C, which indicated specific binding of the CTX moiety to the PANC-1 cell surface (Figure 5).

EEA-1 plays a key role in the clathrin-dependent pathway and contains an FYVE finger, which interacts with PI3K [45, 46]. PI3K phosphorylates Rab5, which helps EEA-1 to localize to early-endocytic compartments [47]. We observed colocalization of M-CTX-Fc with EEA-1 that corresponds to the preliminary step in the endosomal pathway before transfer to the sorting endosomes (Figure 4).

MMP-2 and MMP-9 expression has been correlated with pancreatic cancer cell invasion [48] and local recurrence rate [49]. As mentioned above, activation of MMP-2 and other MMPs and expression of MT1-MMP and $\alpha_v\beta_3$ have been shown to correlate with tumor invasion, neovascularization, and metastasis of glioma [50], melanoma cells both in vitro and in vivo [51], and breast cancer [52]. M-CTX-Fc inhibited cell migration in a dose-dependent manner (Figure 6A). In summary, M-CTX-Fc was shown to inhibit and arrest the cell proliferation machinery without being toxic to the cells.

The findings presented in this study have significant therapeutic implications. M-CTX-Fc markedly inhibited the migration of PANC-1 suggest this drug can be useful in the treatment of pancreatic cancer. Furthermore, CTX has passed preclinical safety studies and has recently won FDA approval for use in a phase I/II clinical trial [20]. Several embryologically-related tumors have also been shown to express MMP-2 and to bind CTX [22]. Clinical use of CTX may thus be expanded to include these tumors as well. However, CTX may have even broader utility as a potentially specific MMP-2 inhibitor. MMP-2 is implicated in a range of diseases that involve tissue remodeling in disease progression. Several chemical inhibitors of MMP-2 are in various stages of clinical testing but most have failed because of toxicity or lack of specificity. CTX may be

a safer and more specific drug, worthy of further exploration in this context. Moreover, the M-CTX-Fc fusion protein may be an effective instrument for targeting MMP-2-expressing cells and drug delivery.

REFERENCES

1. Hariharan D, Saied A, and Kocher HM. Analysis of mortality rates for pancreatic cancer across the world. HPB. 2008; 10: 58–62.
2. Ellenrieder V, Alber B, Lacher U, Hendler SF, Menke A, Boeck W, Wagner M, Wilda M, Friess H, Büchler M, Adler G, and Gress T M. Role of MT-MMPs and MMP-2 in pancreatic cancer progression. Int J Cancer. 2000; 85: 14–20.
3. Destouches D, Huet E, Sader M, Frechault S, Carpentier G, Ayoul F, Briand JP, Menashi S, and Courty J. Multivalent Pseudopeptides Targeting Cell Surface Nucleoproteins Inhibit Cancer Cell Invasion through Tissue Inhibitor of Metalloproteinases 3 (TIMP-3) Release. J Biol chem. 2012; 287: 43685–43693.
4. Yue J, Zhang K, and Chen J. Role of integrins in regulating proteases to mediate extracellular matrix remodeling. Cancer Microenviron. 2012; 5: 275–283.
5. Coussens LM, Fingleton B, and Matrisian LM. Matrix metalloproteinase inhibitors and cancer: trials and tribulations. Science. 2002; 295: 2387–2392.
6. Liotta LA, Steeg PS, and Stetler-Stevenson WG. Cancer metastasis and angiogenesis: an imbalance of positive and negative regulation. Cell. 1991; 64: 327–336.
7. Parks WC, Wilson CL, and López-Boado YS. Matrix metalloproteinases as modulators of inflammation and innate immunity. Nat Rev Immunol. 2004; 4: 617–629.

8. Roomi MW, Ivanov V, Kalinovsky T, Niedzwiecki A, and Rath M. Inhibition of glioma cell line A-172 MMP activity and cell invasion in vitro by a nutrient mixture. Med Oncol. 2007; 24: 231–238.
9. Wild-Bode C, Weller M, and Wick W. Molecular determinants of glioma cell migration and invasion. J Neurosurg. 2001; 94: 978–984.
10. Seiki M. Membrane-type matrix metalloproteinases. APMIS. 1999; 107: 137–143.
11. Sato H, Takino T, Okada Y, Cao J, Shingawa A, Yamamoto E, and Seiki M. A matrix metalloproteinase expressed on the surface of invasive tumor cells. Nature.1994; 370: 61–65.
12. Itoh Y, and Seiki M. MT1-MMP: a Potent Modifier of Pericellular Microenvironment. J cell physiol. 2006; 206: 1–8.
13. Brown PD, Bloxidge RE, Stuart NS, Gatter KC, and Carmichae J. Association between expression of activated 72-kilodalton gelatinase and tumor spread in non-small-cell lung carcinoma. J Natl Cancer Inst. 1993; 85: 574–578.
14. Okada Y, Morodomi T, Enghild JJ, Suzuki K, Yasui A, Nakanishi I, Salvesen G, and Nagase H. Matrix metalloproteinase 2 from human rheumatoid synovial fibroblasts. Purification and activation of the precursor and enzymatic properties. Eur J Biochem. 1990; 194: 721–730.
15. Kinoshita T, Sato H, Takino T, Itoh M, Akizawa T, and Seiki M. Processing of a precursor of 72-kilodalton type IV collagenase/gelatinase A by a recombinant membrane-type 1 matrix metalloproteinase. Cancer Res. 1996; 56: 2535–2538.

16. Sato H, and Takino T. Coordinate action of membrane-type matrix metalloproteinase-1 (MT1-MMP) and MMP-2 enhance pericellular proteolysis and invasion. Cancer Sci. 2010; 101: 843–847.
17. Hernandez-Barrantes S, Toth M, Bernardo MM, Yurkova M, Gervasi DC, Raz Y, Sang QA, and Fridman R. Binding of active (57 kDa) membrane type 1-matrix metalloproteinase (MT1-MMP) to tissue inhibitor of metalloproteinase (TIMP)-2 regulates MT1-MMP processing and pro-MMP-2 activation. J Biol Chem. 2000; 275: 12080–12089.
18. DeBin JA, Maggio JE, and Strichartz GR. Purification and characterization of chlorotoxin, a chloride channel ligand from the venom of the scorpion. Am J Physiol. 1993; 264: 361-369.
19. Mamelak AN, and Jacoby DB. Targeted delivery of antitumoral therapy to glioma and other malignancies with synthetic chlorotoxin TM-601. Expert Opin. Drug Deliv. 2007; 4: 175–186
20. Deshane J, Garner CC, and Sontheimer H. Chlorotoxin inhibits glioma cell invasion via matrix metalloproteinase-2. J Biol Chem. 2003; 278: 4135–4144.
21. Soroceanu L, Gillespie Y, Khazaeli MB, and Sontheimer H. Use of chlorotoxin for targeting of primary brain tumors. Cancer Res. 1998; 58: 4871–4879.
22. Lyons SA, O'Neal J, and Sontheimer, H. Chlorotoxin, a scorpion-derived peptide, specifically binds to gliomas and tumors of neuroectodermal origin. Glia. 2002; 39: 162–173.

23. Jacoby DB, Dyskin E, Yalcin M, Kesavan K, Dahlberg W, Ratliff J, Johnson EW, and Mousa SA. Potent pleiotropic anti-angiogenic effects of TM601, a synthetic chlorotoxin peptide. Anticancer Res. 2010; 30: 39-46.

24. Veiseh M, Gabikian P, Bahrami SB, Veiseh O, Zhang M, Hackman RC, Ravanpay AC, Stroud MR, Kusuma Y, Hansen SJ, Kwok D, Munoz NM, Sze RW, Grady WM, Greenberg NM, Ellenbogen RG, and Olson JM. Tumor paint: a chlorotoxin: Cy5.5 bioconjugate for intraoperative visualization of cancer foci. Cancer Res. 2007; 67: 6882-6888.

25. Sun C, Veiseh O, Gunn J, Fang C, Hansen S, Lee D, Sze R, Ellenbogen RG, Olson J, and Zhang M. In vivo MRI detection of gliomas by chlorotoxin-conjugated superparamagnetic nanoprobes. Small. 2008; 4: 372-379.

26. Veiseh O, Sun C, Fang C, Bhattarai N, Gunn J, Kievit F, Du K, Pullar B, Lee D, Ellenbogen RG, Olson J, and Zhang M. Specific targeting of brain tumors with an optical/magnetic resonance imaging nanoprobe across the blood-brain barrier. Cancer Res. 2009; 69: 6200-6207.

27. Meng XX, Wan JQ, Jing M, Zhao SG, Cai W, and Liu EZ. Specific targeting of gliomas with multifunctional superparamagnetic iron oxide nanoparticles optical and magnetic resonance imaging contrast agents. Acta Pharmacol Sin. 2007; 28: 2019-2026.

28. Veiseh O, Kievit FM, Gunn JW, Ratner BD, and Zhang M. A ligand-mediated nanovector for targeted gene delivery and transfection in cancer cells. Biomaterials. 2009; 30: 649-657.

29. Kasai T, Nakamura K, Vaidyanath A, Chen L, Sekhar S, El-Ghlban S, Okada M, Mizutani A, Kudoh T, Murakami H, and Seno M. Chlorotoxin Fused to IgG-Fc Inhibits Glioblastoma Cell Motility via Receptor-Mediated Endocytosis. J drug deliv. 2012.
30. Hashizume T, Fukuda T, Nagaoka T, Tada H, Yamada H, Watanabe K, Salomon DS, and Seno M. Cell type dependent endocytic internalization of ErbB2 with an artificial peptide ligand that binds to ErbB2. Cell Biol Int. 2008; 32: 814–826.
31. Hagemann T, Robinson SC, Schulz M, Trümper L, Balkwill FR, and Binder C. Enhanced invasiveness of breast cancer cell lines upon co-cultivation with macrophages is due to TNF-alpha dependent up-regulation of matrix metalloproteases. Carcinogenesis. 2004; 25: 1543-1549.
32. Mayor S, Pagano RE. Pathways of clathrin-independent endocytosis. Nat Rev Mol Cell Biol. 2007; 8: 603–12.
33. Kirkham M, Parton RG. Clathrin-independent endocytosis: new insights into caveolae and non-caveolar lipid raft carriers. Biochim Biophys Acta. 2005; 1745: 273–86.
34. Falcone S, Cocucci E, Podini P, et al. Macropinocytosis: regulated coordination of endocytic and exocytic membrane traffic events. J Cell Sci. 2006; 119: 4758–69.
35. Gong YL, Xu GM, Huang WD, and Chen LB. Expression of matrix metalloproteinases and the tissue inhibitors of metalloproteinases and their local invasiveness and metastasis in Chinese human pancreatic cancer. J Surg Oncol. 2000; 73: 95–9.

36. Gress TM, Müller-Pillasch F, Lerch MM, Friess H, Büchler M, and Adler G. Expression and in situ localization of genes coding for extracellular matrix proteins and extracellular matrix degrading proteases in pancreatic cancer. Int J Cancer 1995; 62: 407–13.
37. Yamamoto H, Itoh F, Iku S, Adachi Y, Fukushima H, Sasaki S, Mukaiya M, Hirata K, and Imai K. Expression of matrix metalloproteinases and tissue inhibitors of metalloproteinases in human pancreatic adenocarcinomas: Clinicopathologic and prognostic significance of matrilysin expression. J Clin Oncol. 2001; 19: 1118–27.
38. Hofmann UB, Westphal JR, Kraats AA, Ruiter DJ, and Muijen GN. Expression of integrin αvβ3 correlates with activation of membranetype matrix metalloproteinase-1 (MT1-MMP) and matrix metalloproteinase-2 (MMP-2) in human melanoma cells in vitro and in vivo. Int. J. Cancer. 2000; 87:12–19.
39. Deryugina EI, Ratnikov B, Monosov E, Postnova TI, DiScipio R, Smith JW, and Strongin AY. MT1-MMP initiates activation of proMMP-2 and integrin αvβ3 promotes maturation of MMP-2 in breast carcinoma cells. Exp Cell Res. 2001; 263: 209–223.
40. Nagase H. Cell surface activation of progelatinase A (proMMP-2) and cell migration. Cell Res. 1998; 8: 179–86.
41. Strongin AY, Collier I, Bannikov G, Marmer BL, Grant GA, and Goldberg GI. Mechanism of cell surface activation of 72-kDa type IV collagenase. Isolation of the activated form of the membrane metalloprotease. J Biol Chem. 1995; 270: 5331–5338.

42. McFerrin MB, Sontheimer H. A role for ion channels in glioma cell invasion. Neuron Glia Biol. 2006; 1: 39-49.

43. Osenkowski P, Toth M, and Fridman R. Processing, shedding, and endocytosis of membrane type 1-Matrix metalloproteinase (MT1-MMP). J Cell Physiol. 2004; 200: 2–10.

44. Gálvez BG, Matías-Román S, Yáñez-Mó M, Sánchez-Madrid F, and Arroyo AG. ECM regulates MT1-MMP localization with β1 or αvβ3 integrins at distinct cell compartments modulating its internalization and activity on human endothelial cells. Journal of Cell Biology. 2002; 159: 509–521.

45. Mu FT, Callaghan JM, Steele-Mortimer O, Stenmark H, Parton RG, Campbell PL, McCluskey J, Yeo JP, Tock EP, and Toh BH. EEA1, an early endosome-associated protein. EEA 1 is a conserved alpha-helical peripheral membrane protein flanked by systeine "fingers" and contains a calmodulin-binding IQ motif. J Biol Chem. 1995; 270: 13503–11.

46. Mills IG, Jones AT, and Clague MJ. Involvement of the endosomal autoantigen EEA1 in homotypic fusion of early endosomes. Curr Biol. 1998; 8: 881– 4.

47. Sönnichsen B, De Renzis S, Nielsen E, Rietdorf J, and Zerial M. Distinct membrane domains on endosomes in the recycling pathway visualized by multicolor imaging of Rab4, Rab5, and Rab 11. J Cell Biol. 2000; 149: 901–14.

48. Yang X, Staren ED, Howard JM, Iwamura T, Bartsch JE, Appert HE. Invasiveness and MMP expression in pancreatic carcinoma. J Surg Res. 2001; 98: 33-9.

49. Koshiba T, Hosotani R, Wada M, Miyamoto Y, Fujimoto K, Lee JU, Doi R, Arii S, and Imamura M. Involvement of matrix metalloproteinase-2 activity in invasion and metastasis of pancreatic carcinoma. Cancer. 1998; 82: 642-50.

50. Bello L, Lucini V, Carrabba G, Giussani C, Machluf M, Pluderi M, Nikas D, Zhang J, Tomei G, Villani RM, Carroll RS, Bikfalvi A, and Black PM. Simultaneous inhibition of glioma angiogenesis, cell proliferation and invasion by a naturally occurring fragment of human metalloproteinase-2. Cancer Res. 2001; 61: 8730–8736.

51. Hofmann UB, Westphal JR, Waas ET, Becker JC, Ruiter DJ, and Van Muijen GN. Coexpression of integrin alpha(v)beta3 and matrix metalloproteinase-2 (MMP-2) coincides with MMP-2 activation: correlation with melanoma progression. J Invest Dermatol. 2000; 115: 625–632.

52. Deryugina EI, Bourdon MA, Jungwirth K, Smith JW, and Strongin AY. Functional activation of integrin αvβ3 in tumor cells expressing membrane type 1 matrix metalloprotease. Int. J. Cancer. 2000; 86: 15–23.

CHAPTER 3

Antitumor Effect of Novel Doxorubicin Loaded Liposomes Modified with Chlorotoxin-Fc Protein against Human Pancreatic Cancer Cells

ABSTRACT

The monomeric form of Chlorotoxin (M-CTX-Fc), the fusion protein was generated by joining the CTX peptide to the amino terminus of the human IgG-Fc domain without a hinge domain, binding to pancreatic cancer with high specificity, was firstly applied to establish the M-CTX-Fc modified DOX loaded liposome delivery system for targeting the PANC-1 cells and improving the antitumor efficacy. The physicochemical characterization of the novel liposome system presented a satisfactory size of 100 nm with uniform distribution, high encapsulation and adequate drug loading capacity of anticancer drug (DOX). Cellular association and internalization studies revealed that attachment of M-CTX-Fc onto the liposomal surface enhanced particle internalization into PANC-1 cells. *In vitro* cytotoxicity studies proved that the presence of M-CTX-Fc increased the cytotoxicity against the PANC-1 cells compared with non-modified liposomes. In BALB/c mice bearing PANC-1 tumor, the M-CTX-Fc modified liposome treatment slowed tumor growth more significantly than non-modified liposome. The immunohistochemical studies showed a decrease in Ki67 and CD31 staining in tumor cells from DOX-SSL-M-CTX-Fc treated mice when compared with PBS-treated groups, which suggests an inhibition of tumor proliferation rate and angiogenic process associate with tumor growth. The M-CTX-Fc modified liposome did not cause the unexpected side effects and could be used as safe drug carriers.

1. INTRODUCTION

Pancreatic cancer is the fourth most common cause of cancer-related mortality worldwide [1] and is characterized by local invasion, early metastasis, and a strong desmoplastic reaction [2]. Matrix metalloproteinases (MMPs) are a family of enzymes that proteolytically degrade various components of the extracellular matrix (ECM). Angiogenesis is the process of forming new blood vessels from existing ones and requires degradation of the vascular basement membrane and remodeling of the ECM in order to allow endothelial cells to migrate and invade into the surrounding tissue. MMPs participate in this remodeling of basement membranes and ECM. However, it has become clear that MMPs contribute more to angiogenesis than just degrading ECM components. Specific MMPs have been shown to enhance angiogenesis by helping to detach pericytes from vessels undergoing angiogenesis, by releasing ECM-bound angiogenic growth factors, by exposing cryptic proangiogenic integrin binding sites in the ECM, by generating promigratory ECM component fragments, and by cleaving endothelial cell-cell adhesions [3-5].

For these purpose, molecules that inhibit matrix metalloproteinase (MMP) activity or induce the expression of their natural inhibitors, the tissue inhibitor of metalloproteinases (TIMPs), are potentially interesting [6]. Among the MMPs, MMP-2 (gelatinase A) and MMP-9 (gelatinase B) are different from the others because of their ability to degrade gelatin and type IV collagen, the main component of the extracellular matrix (ECM), which is the main barrier separating in situ and invasive carcinoma [7].

Chlorotoxin (CTX) is a 36-amino acid peptide which contains four disulfide bridges and is derived from *Leiurus quinquestriatus* (scorpion) venom. Early studies demonstrated that CTX can inhibit a potentially glioma-specific chloride ion channel [8]. CTX is believed to bind a lipid raft-anchored complex that contains MMP-2 [9], membrane type-1 MMP, tissue inhibitor of metallopreotease-2 [10], and other proteins [11]. In addition to glioma cells, CTX has been shown to specifically bind to other tumors of neuroectodermal origin [12]. It was recently found that CTX not only binds a wide range of tumor cell types but is also internalized by proliferating human vascular endothelial cells [13]. These studies also demonstrated an anti-angiogenic effect of chlorotoxin using both the chicken chorioallantoic membrane assays and mouse matrigel plug assays. Notably, chlorotoxin inhibited angiogenesis induce by a wide range of stimuli including, VEGF, bFGF, hepatocytes growth factor, PDGF-AB, tumor necrosis factor-α, and interleukin-6. Chlorotoxin was also able to specifically inhibit angiogenesis stimulated by several different types of implanted tumor [13]. Using affinity purification followed by mass spectrometry, MMP-2 was demonstrated to be the receptor of chlorotoxin [14].

CLTx has been used in glioma imaging of animals bearing xenografted tumors by tagging CY5.5 or iodine-131 to ClTx, [15, 16] and iodine-131-tagged ClTx-modifided nanoparticles also have demonstrated great potential in gene therapy and glioma chemical therapy [17]. We have previously reported CTX-dependent inhibition of proliferation and motility in glioblastoma cells using a targeted bionanocapsule displaying the monomeric fusion protein of chlorotoxin (M-CTX-Fc). Moreover, M-CTX-Fc had a more efficient inhibitory effect on migration than CTX. We observed cellular uptake of the

bionanocapsules, indicating M-CTX-Fc is an effective vehicle as a drug delivery system [18].

Also, we reported that M-CTX-Fc decreased MMP-2 release into the media of PANC-1 cells in a dose-dependent manner. M-CTX-Fc internalization into PANC-1 cells was observed. When the cells were treated with chlorpromazine (CPZ), the internalization of the fusion protein was reduced, implicating a clathrin-dependent internalization mechanism of M-CTX-Fc in PANC-1 cells. Furthermore, M-CTX-Fc clearly exhibited the inhibition of the migration depending on the concentration. The M-CTX-Fc may be an effective instrument for targeting pancreatic cancer [19]. All these data raise the possibility that M-CTX-Fc could more broadly be used to specifically deliver conjugated cytotoxic drugs to tumors. Thus, it is necessary to evaluate whether the M-CTX-Fc-modified liposomes could target the pancreatic cancer and further increase the antitumor effect via increasing uptake in tumor cells and hence has an antitumor effect on pancreatic cancer.

To realize this strategy, we established the targeted liposomes conjugated to the monomeric form of chlorotoxin (M-CTX-Fc) and entrapped with DOX. After the delivery system was characterized, the targeting capability of M-CTX-Fc modified liposome was studied *in vitro* on the tumor model of PANC-1 (pancreatic cancer) cells. The *in vivo* targeting efficiency and antitumor activity of M-CTX-Fc modified liposome were evaluated on the tumor models of PANC-1 pancreatic bearing nude mice.

2. MATERIALS AND METHODS

2.1. Materials

1,2-Dipalmitoyl-sn-glycero-3-phosphocholine (DPPC) was purchased from NOF Corporation (COATSOME), cholesterol (Chol) was from (KANTO chemical), N-[(3-Maleimide-1-oxopropyl) aminopropyl polyethyleneglycol-carbamyl] distearoylphosphatidyl-ethanolamine (DSPE-PEG-Mal) and N-(Carbonyl-methoxypolyethyleneglycol2000)-1,2-distearoyl-sn-glycero-3-phosphoeth-anolamine, sodium salt were purchased from NOF Corporation (SUNBROIGHT, Tokyo, Japan), 2-iminothiolane hydrochloride and human IgG were from (Sigma), Doxorubicin hydrochloride was from (Wako), Amicon Ultra was obtained from (MerckMilipore Ltd), and PD 10 columns was purchased from (GE Healthcare).

2.2. Cell Culture and animals

The human cell line derived from pancreatic carcinoma, PANC-1 (RCB2095), was provided by the National BioResource Project of MEXT, Japan. The cells were grown and subcultured in RPMI medium (Sigma-Aldrich, St Louis, MO, USA) supplemented with 10% fetal bovine serum (FBS, PAA Laboratories, Pasching, Austria) in the presence of 100 IU/mL penicillin and 100 μg/mL streptomycin (Nacalai Tesque, Kyoto, Japan). The cells were maintained at 37°C in a humidified incubator with 95% air and 5% CO_2.

Nude mice (BALB/c -nu/nu, 6 weeks) were purchased from Charlesriver, Japan. The plan of animal experiments was reviewed and approved by the ethics committee for animal experiments of Okayama University.

2.3. Expression and Purification of M-CTX-Fc

The preparation of M-CTX-Fc was performed as previously described [18]. *Escherichia coli* BL21 (DE3) pLysS (Novagen) was transformed with the expression vector for M-CTX-Fc. After induction of the expression vector, the transformant was cultured and the bacteria were harvested. The inclusion bodies were washed and then were dissolved in 6 M guanidinium-HCl containing 0.1 M Tris-HCl (pH 8.5). The protein in the solution was reduced and then refolded. The solution containing refolded protein was purified using a cobalt resin column (Talon super flow metal affinity resin, Clontech, Mountain View, CA, USA). The eluted solution was dialyzed thrice using phosphate-buffered saline (Dulbecco's formula, hereafter PBS). The purity of M-CTX-Fc in the final preparation was assessed by sodium dodecyl sulphate-polyacrylamide gel electrophoresis (SDS-PAGE), Coomassie Brilliant Blue (CBB) staining, and western blotting.

2.4. Preparation of liposomes

Nanoliposomes were prepared in the three formulations: (1) DOX-Loading liposomes modified with M-CTX-Fc, (2) DOX-Loading liposomes modified with human IgG, (3) non-modified liposomes loading DOX. These liposomes were basically composed of DPPC/Chol/ m-DSPE-PEG.

2.4.1. Preparation of DOX-loading liposomes

Lipids of DPPC/Chol powders were mixed at a molar ratio of (3:1) with 5 mole % of m-DSPE-PEG and were dissolved in a Chloroform/Methanol (9:1) mixture in a round bottomed flask. Chloroform/methanol mixture was evaporated using rotary evaporator

(EYELA, N-1200A) and the lipid thin film was obtained. The lipid film was incubated under vaccum overnight to remove the remaining organic solvent and form dried film. At the next step, 2 mL of 0.8 mg/mL of Doxorubicin hydrochloride at 50°C was added to the dried film and vortex-mixed vigorously for 30 min to obtain dispersion. Primary homogenization was performed by prob sonicators (astrason 3000) for 3 min at 60°C. Un-entrapped DOX was removed from the liposome suspensions by centrifugation and the liposome pellet was washed three times with PBS (pH 7.4).

2.4.2. Preparation of DOX- loading liposomes modified with M-CTX-Fc or human IgG

M-CTX-Fc coupled (modified) DOX-loading liposomes were prepared by the postinsertion method (20, 21). Briefly, M-CTX-Fc was modified with the addition of thiol groups upon reaction with freshly prepared 2-iminothiolane hydrochloride (2-IT) at a molar ratio 1:10 (M-CTX-Fc: 2-IT), in HEPES-buffered saline (HBS, 25 mM HEPES, 140 mM NaCl, pH 8.0). The reaction occurred under gentile stirring for 1 h in the dark at room temperature. Unreacted 2-IT reagent was removed by chromatography on a PD 10 column with HBS (pH 7.4). Thiolated M-CTX-Fc was then coupled to Mal-DSPE-PEG micelles, prepared in HBS (pH 7.4) by a thioether linkage. The coupling reaction was performed overnight in the dark with gentle stirring.

DOX-SSL-IgG Liposomes were prepared in the same way as DOX-SSL-M-CTX-Fc except that human IgG was thiolated by 2-iminothiolane at a molar ratio 1:50 (human IgG: 2-IT).

2.5. Characterization of liposomes

2.5.1. Size distribution and zeta potential

The particle size and zeta potential of liposomes were determined by dynamic light scattering (DLS) analysis using ELS-8000 Electrophoretic light scattering (Photal, OTSUKA Electronics) at 25 °C. The data for each sample were obtained in three measurements.

2.5.2. Encapsulation efficiency (EE) and loading efficiency (LE)

The concentration of DOX was quantified by UV–VIS-spectrophotometry at 490 nm. The encapsulation efficiency (EE) and the drug loading Efficiency (LE) were calculated using the following calculations: EE (%) = drug loaded/total drug × 100%; LE (%) = drug loaded/total materials × 100%.

2.5.3. Mesurement of lipid concentration

The total lipid concentration was assessed by chlolesterol quantification, using Tcho E kit (wako). The absorbance was measured at 600 nm in a spectrophotometer and the concentration was determined from a standard curve for cholesterol content.

2.5.4. Quantification of M-CTX-Fc conjugated to the liposome

2.5.4.1. Enzyme-linked immunosorbent assay (ELISA).

The amount of M-CTX-Fc on the surface of the liposome was measured by enzyme-linked immunosorbent assay (ELISA). 100 µg/mL of M-CTX-Fc was diluted with PBS to a final concentration in a range of 6.25-100 ng/mL (standard solution). One hundred microliters of standard solution and liposomes modified with M-CTX-Fc were added to each well of a 96-well ELISA plate (REF 655061) and maintained overnight at 4°C for

immobilization. After discarding the solution of each well, 150 μL of TBST containing 10% skim milk was added to each well for blocking and incubated at 25°C for 2 h. Each well was then washed five times with TBST. Next, 150 μL of protein A conjugated with HRP (KPL, cat. No. 14-50-00) diluted 6000-fold with TBST containing 0.05% Tween20 was added to each well and stood at 25°C for 1 h. After five washes with TBST, 100 μL of TMB Stabilized Substrate for HRP (Promega) was added to each well and reacted at 25°C for 30 min and then 50 μL of 1 N sulfuric acid was added to each well to stop the reaction. The absorbances of standards and samples were measured at 450 nm using a microplate-reader (BioRad). The binding reactions of M-CTX-Fc were repeated three times and the results were expressed as mean ± SD.

2.5.4.2. Western blotting

The amount of M-CTX-Fc on the surface of the liposome was confirmed by western blotting. Fifteen microliters of 25, 50, 100, and 200 μg/ml of M-CTX-Fc were suspended in Laemmli buffer with β-mercaptoethanol, heated for 5 min at 95°C, and finally processed for subjected to SDS-PAGE and western blotting. Proteins resolved on SDS-PAGE were transferred to a polyvinylidene difluoride (PVDF) membrane (Millipore, Billerica, MA, USA). The membrane was blocked with 10% skim milk in 10 mM Tris-HCl (pH 7.4), 150 mM NaCl containing 0.1% Tween-20 (TBST). The blots were probed with anti-human IgG mouse monoclonal antibody conjugated with HRP (Life Technologies, Carlsbad, CA, USA) diluted to 1:1000 in TBST containing 10% skim milk. The HRP signal was developed using a Western Lightning Plus-ECL chemiluminescence reagent (PerkinElmer, Waltham, MA, USA), and the intensities of the bands were visualized using a Light-

Capture II cooled CCD camera system (ATTO, Tokyo, Japan). Quantitative assessments of the intensity of the blots were analyzed using Image J.

2.6. DOX accumulation in cells

Cellular accumulation of DOX was measured as described by Chambers et al. [22] with slight modifications. 10^6 cells were seeded in 35-mm plates. The cells were incubated with free DOX or DOX loaded in the liposomes, 1-10 μg/mL, for 2 h at 37°C. The cells were rinsed three times with ice-cold PBS and the drug was extracted from the cells with l ml acidified isopropanol (0.075 M HCI in 90% isopropanol), for 20 h at 4°C. DOX concentration was determined spectrofluorometrically using an excitation wavelength of 490 nm and an emission wavelength of 590 nm. The fluorescence intensity emitted was translated into DOX-equivalents based on a DOX standard curve, after readings of untreated background cells were subtracted. Cell-associated DOX was expressed as ng DOX/10^6 cells.

2.7. Fluorescence detection

PANC-1 cells were grown on 18-mm cover slips (Iwaki, Tokyo, Japan) in 12-well plates. The cells were incubated with 300 nM of M-CTX-Fc conjugated with DOX-SSL-CTX-Fc and 300 nM of IgG conjugated with DOX-SSL-IgG in PBS containing 1% BSA for 1h at 37°C. The cells were washed twice with PBS to evaluate specific binding to cell surfaces. The cells were fixed with 4% paraformaldehyde in PBS, permeabilized with 0.2% Triton X-100, and blocked with a blocking solution containing 1% BSA in PBS. The cells were washed with PBS and incubated with FITC-labeled anti-human IgG-Fc antibody

(Sigma-Aldrich) for 1 h at 25°C. After further washes, the nuclei were stained with DAPI (Vector Laboratories Inc., Burlingame, CA, USA), and the cells were visualized and photographed using Olympus IX81 microscope equipped with a light fluorescence device (Olympus, Japan).

2.8. In vitro cytotoxicity assay

The 3-(4, 5-dimethylthiazol-2-yl)-2, 5-diphenyltetrazolium bromide (MTT) colorimetric assay was applied to investigate the *in vitro* efficacy of various DOX-loaded liposomes and free DOX on the cytotoxicity of PANC-1 tumor cells. In brief, the cells were seeded at a density of 5×10^3 cells/well in 96-well plates in RPMI medium supplemented with 10% FBS for 24 h. Then, the cells were incubated with free DOX or different liposome formulations of serial DOX concentrations at 37°C in 5% CO_2 atmosphere for 72 h. The cells were exposed to 5 mg/mL MTT in PBS at a final concentration of 1 mg/mL in culture for 5 h. Formazan crystals formed during the incubation period were dissolved overnight at 37°C by adding 10% SDS containing 20 mM HCl. The absorbance was measured at 570 nm.

2.9. Time dependent inhibition (IT_{50}) assay

The time required for 50% growth inhibition was estimated using MTT assay. Briefly, cells were plated in 96-well flat bottom tissue culture plates at 5000 cells/well and incubated at 37°C in a 5% CO_2 incubator for 24 h, which provided sufficient time for cells to attach and resume growth. The concentration of DOX and DOX loaded in the liposomes which inhibited 100% of growth was added to the cells. Then, 1, 2, 3, 6, 12, 24, 48, and 72

h later, the medium containing the drug was removed by aspiration, and each well was washed twice by PBS, fresh medium was added. MTT dye was added to each well at a final concentration of 1 mg/mL for 5 h. Formazan crystals formed during the incubation period were dissolved overnight at 37°C by adding 10% SDS containing 20 mM HCl. The absorbance was measured at 570 nm.

2.10. *In vivo* inhibition of tumor growth.

The BALB/c mice bearing tumors were prepared by injecting 1 X 10^6 cells suspended in 200 μL of culture medium without FBS into the subcutaneous dorsa of the mice. The tumor size was measured with a vernier caliper, and the tumor volume was calculated as V (mm^3) = 0.5 × (the longest diameter) × (the shortest diameter)^2. When the tumor volume reached approximately 50-100 mm^3 (10 days after inoculation), the mice were randomly divided into 6 groups PBS, DOX-SSL and DOX-SSL-M-CTX-Fc, DOX-SSL-IgG, M-CTX-Fc, and combined (DOX-SSL+ M-CTX-Fc). Mice were administered via tail vein at the dosage of 10 mg DOX/kg body weight every 6 days for 3 times. The mice in the saline group were injected with 200 μL of saline as a control and the mice in M-CTX-Fc group were injected with 200 μL of 1.5 mg M-CTX-Fc/Kg. During the process of the treatment, the tumor volumes and body weight were measured every 3 days. Data were represented as a relative tumor volume at the indicated times normalized by that when liposomes were injected at day 1. After *in vivo* anti-tumor treatment, mice were sacrificed and heart, liver, spleen, lung, kidney were collected for histological analysis. The tumors and tissues excised from each group were fixed in 10 % formalin (Wako), embedded in paraffin and

sectioned. Finally, the sections were stained with hematoxylin and eosin (H&E) and observed using an optical microscope.

2.11. Immunohistochemistry (IHC)

IHC for CD31, Ki67 was performed using formalin-fixed paraffin embedded tissue sections and standard procedures. Briefly, 6 mm tissue sections were deparaffinized and antigen retrieved was performed using microwave exposure at 95°C for 10 minutes in a citrate buffer (pH 6.0). After hydrogen peroxide blocking and normal serum blocking, the sections were then incubated for 1 h at 37°C with the following primary antibodies: rabbit polyclonal anti-Ki67 (1:200, Abcam), mouse monoclonal anti-CD31 (1:200, Cell Signaling). The sections were then incubated with biotinylated anti-rabbit, or biotinylated anti-mouse secondary antibody (Vector, USA), followed by incubation with the ABC reagent (Vector, USA). Detection was accomplished using 3, 30-diaminobenzidine tetrahydrochloride (DAB, Vector, USA). Counter staining were carried out using hematoxylin.

2.12. Statistical Analysis.

All the experiments were repeated at least three times. Data are shown as the means ± standard deviation (SD). Student's t test was used to determine the difference. P values less than 0.05 were considered statistically significant.

3. RESULTS AND DISCUSSION

3.1. Preparation and characterisation of DOX-loaded liposomes

The thiolated M-CTX-Fc was easily conjugated with the Mal-PEG2000-DSPE by forming the thiol–ether bond between the thiol and maleimide groups. This thiol–ether bond did not easily hydrolyze *in vivo*, thus maintaining the stability of M-CTX-Fc-PEG2000-DSPE. The Mal-PEG2000-DSPE was incorporated into the lipid bilayers of liposomes through a simple incubation process while the particle size of liposome was not significantly changed. The steric barrier imposed by PEG inhibits the interaction of liposomes with the endosomal membrane, which is essential for endosomal membrane destabilization and the subsequent release of the entrapped DOX. In this regard, our results indicate that incorporation of 5 mole % of m-DSPE-PEG in the developed formulation allows liposomal size stability.

The characteristic of DOX-loaded liposomes modified with M-CTX-Fc or human IgG or not are summarized in Table 1. It was shown that DOX-loaded liposomes were about 88 nm with a polydispersity index (PDI) 0.210, while both M-CTX-Fc or IgG modified DOX-loaded liposomes were slightly larger than non-modified ones with mean particle size 99.8, 99.65 and the low PDI 0.228, 0.204 respectively (Table 1). The dynamic light scattering analysis revealed that the particle size of M-CTX-Fc modified liposomes was about 100 nm (Fig. 1 B). The good particle size uniformity was important since it would not result in significant difference in the receptor-mediated endocytosis of intracellular delivery for the nano-carrier system [23, 24]. It is well known that the particle size plays an important role on the alteration of pharmacokinetics by affecting the tissue

distribution and clearance. Vehicles with small particle size (< 200nm) are known to increase the accumulation of drug in the tumor via enhanced permeability and retention (EPR) effect, although this behavior is dependent on the tumor type [25, 26]. An increase in particle size of liposomes generally results in rapid uptake by the reticuloendothelial system (RES) with rapid clearance and a short half-life. Thus, controlling and maintaining liposomes at small and uniform sizes is a critical in developing a viable pharmaceutical product.

All the liposome formulations had slightly negative charges. The negatively charged surface of the liposomes was designed to avoid being bound by blood proteins, such as opsonin, as well as to enhance the retention in the blood. It was found that more than 90% of DOX could be loaded into liposomes (Table 1).

The presentation and amount of M-CTX-Fc on the surface of liposome was measured by western blotting (Figure 2A and Figure 2B) and enzyme linked immunosorbent assay, ELISA (Figure 2C). 5.7 ± 0.26 nmol M-CTX-Fc per liposome were obtained.

Table 1: Characteristics of three DOX-loading lipoosmes formulations.

Formulations	Diameter (nm)	PD index	Zeta potential (-mV)	Encapsulation efficiency %	Loading efficiency %
DOX-SSL	88.2 ± 3.7	0..21 ± 0.03	5.5 ± 2.7	93.2 ± 1.7	4.1 ± 0.1
DOX-SSL-IgG	99.8 ± 2.6	0.23 ± 0.01	6.2 ± 1.4	92.9 ± 2	4.1 ± 0.08
DOX-SSL-M-CTX-Fc	99.7 ± 7.4	0.20 ± 0.02	5.0 ± 2.4	90.5 ± 2.3	4.9 ± 0.11

Data were presented as the mean±SD.

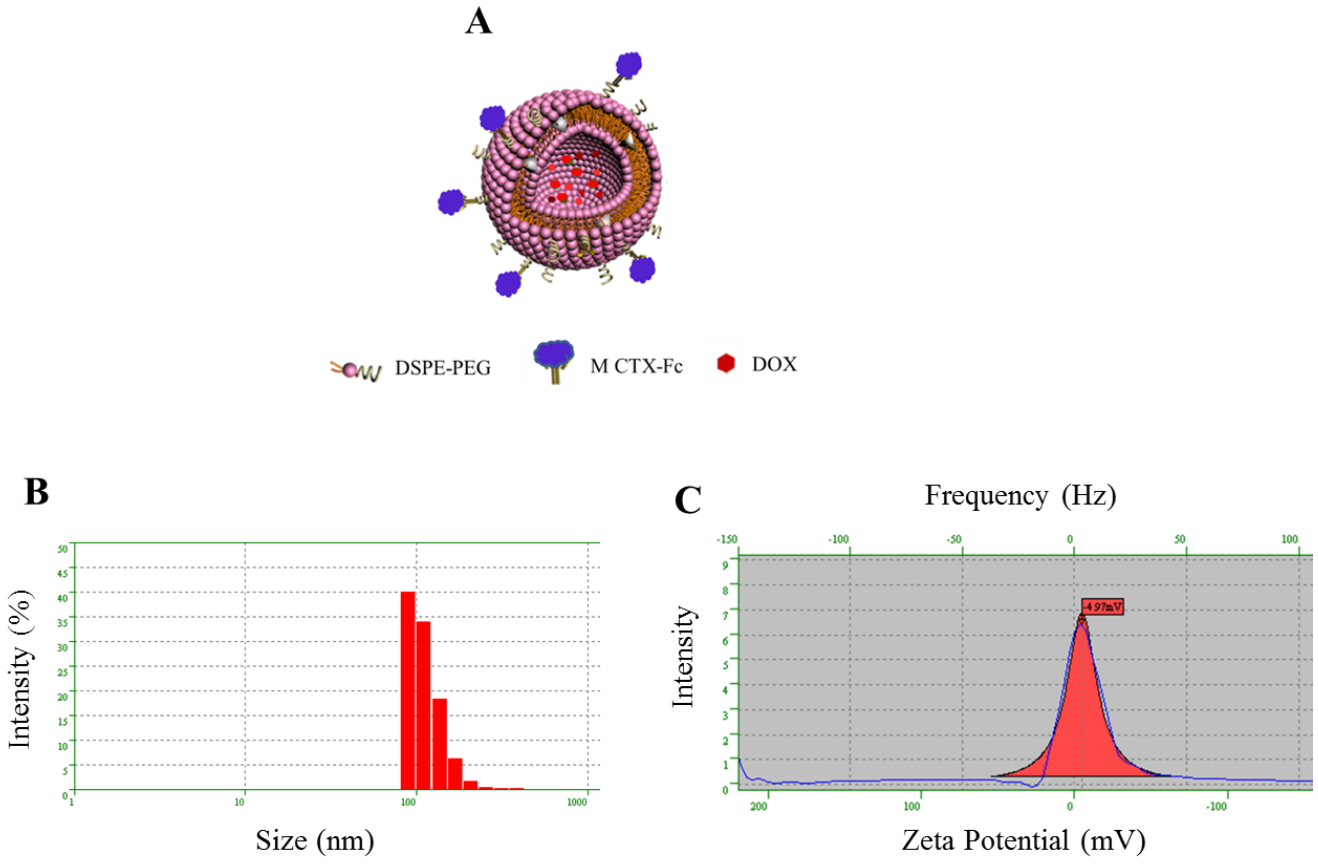

Figure 1: (A) Schematic diagram of DOX-Loaded liposomes modified with M-CTX-Fc. **(B)** Particle size distribution of DOX-SSL-M-CTX-Fc by intensity measured by electrophoretic light scattering in PBS buffer (PH 7.4). **(C)** Zeta potential of DOX-SSL-M-CTX-Fc measured by electrophoretic scattering in PBS

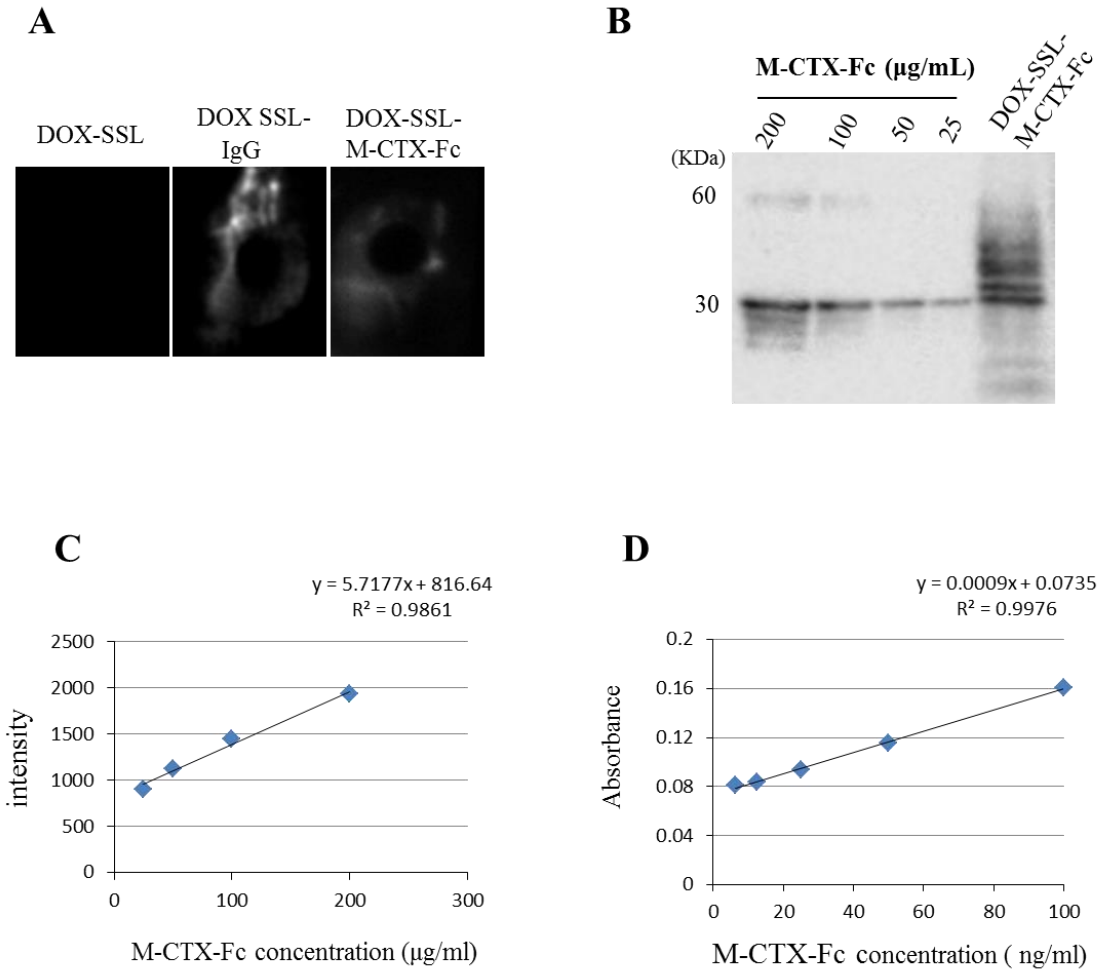

Figure 2: Quantification of M-CTX-Fc conjugated to the liposome. **(A)** 3 µL of DOX-SSL, DOX-SSl-IgG, and DOX-SSL-M-CTX-Fc were added to a PVDF membrane and probe with anti-human IgG mouse monoclonal antibody conjugated with HRP **(A)** the amount of M-CTX-Fc on the surface of liposome was measured by western blotting. **(B)** Quantitative assessments of the intensity of the blots were analysed using image J. **(C)** the standard curve of M-CTX-Fc measured by enzyme linked immunosorbent assay (ELISA).

3.2. Cytotoxicity assay

The *in vitro* IC_{50} values for DOX, DOX-SSL, DOX-SSL-IgG and DOX-SSL-M-

CTX-Fc are presented in table 2. After being incubated with DOX, DOX-SSL, DOX-SSL-IgG, and DOX-SSL-M-CTX-Fc for 72 h, the PANC-1cell viability was obviously inhibited. The inhibition increased as the concentration of DOX or the equivalent concentration of DOX loaded in the liposomes increased. The free DOX showed greatest cytotoxicity with lowest IC_{50} (IC_{50} = 0.59 μg/mL) against PANC-1 cells. Similarly, compared to non-modified liposomes, the M-CTX-Fc modification exhibited higher cytotoxicity against PANC-1 cells. After 72 h, the IC_{50} values of DOX-SSL were 3.23 fold as much as those of DOX-SSL-M-CTX-Fc. The viability of cells treated with free DOX decreased sharply because DOX molecule diffused directly into cells. The endocytosis of liposomes was slower than the cellular uptake of free DOX, so at the same concentration, free DOX produced higher cytotoxicity compared with the DOX-SSL (IC_{50} = 3.43 μg/mL), DOX-SSL-CTX-Fc (IC_{50} = 1.06 μg/mL) displayed higher growth inhibition (Table 2).

Table 2: IC_{50} and IT_{50} of DOX and the different DOX-loading liposomes formulations against PANC-1 cells.

Formulations	IC_{50} (μg/mL)	IC_{100} (μg/mL)	IT_{50} (h)
DOX	0.59 ±0.05	2.3 ±0.12	1.2 ± 0.12
DOX-SSL	3.4 ± 0.14	7.5 ±0.2	3.9 ± 0.2
DOX-SSL-IgG	> 10	-	-
DOX-SSL-M-CTX-Fc	1.1 ± 0.08	4.6 ±0.24	1.7 ± 0.23

Data were presented as the mean±SD.

3.3. Cellular uptake

To investigate the reason for the increased toxicity of free DOX compared to non-modified or modified M-CTX-Fc liposomes, we examined the cellular uptake of DOX in PANC-1 cells (figure 3). The cellular fluorescence intensity of the DOX reflected the cellular uptake behavior of the liposomes. In all cases, there was a linear correlation between the amount of cell-associated drug and the drug concentration in the medium within the tested range. The amount of drug associated with PANC-1 cells was 5 fold less when the drug was presented in liposome. As shown in (figure 3), the intracellular DOX in the DOX-SSL-M-CTX-Fc was higher than the DOX-SSL. In detail, the amount of DOX associated with the cells which were incubated with DOX-SSL-M-CTX-Fc was 1.6 times as high as that of DOX-SSL. The higher uptake of DOX-SSL-M-CTX-Fc compared to DOX-SSL suggested more or easy endocytosis due to the presence of specific binding. In contrast without the modification on liposomes, the non-specific and endocytosis were very low binding, and this in the case of DOX-SSL. In addition, the uptake of free DOX was the highest due to the direct diffusion into the cells. Therefore, the free DOX showed the greatest cytotoxicity against PANC-1 cells, which was consistent to its maximum cellular uptake. M-CTX-Fc modification could increase the cytotoxicity of liposomes likely due to the high cellular uptake of DOX. Consequently, M-CTX-Fc facilitated the binding and internalization, and targeting efficiency of liposomes to the related tumor cells and endothelial cells in the study.

3.4. Microscope studies

(Figure 4) exhibits the intracellular accumulation and distribution of DOX entrapped

by PANC-1 cells using Olympus IX81 microscope. When the cells were incubated with M-CTX-Fc modified liposomes at 4°C, the fluorescence from FITC-labeled antihuman IgG indicated localization of the fused proteins on the plasma membrane. However, when the cells were incubated at 37°C, the fluorescence indicated that M-CTX-Fc was localized intracellularly in PANC-1 cells (Figure 4). M-CTX-Fc modified liposomes showed more obvious intracellular green fluorescence from FITC-labeled antihuman IgG than IgG modified liposomes whose fluorescence could be hardly identified, especially in the nuclei. The IgG modified liposomes produced no fluorescence at 37°C indicating the specific of CTX moiety to PANC-1 cell surface. It was clear suggested here that M-CTX-Fc could markedly improve the recognition and uptake of liposomes by PANC-1 cells.

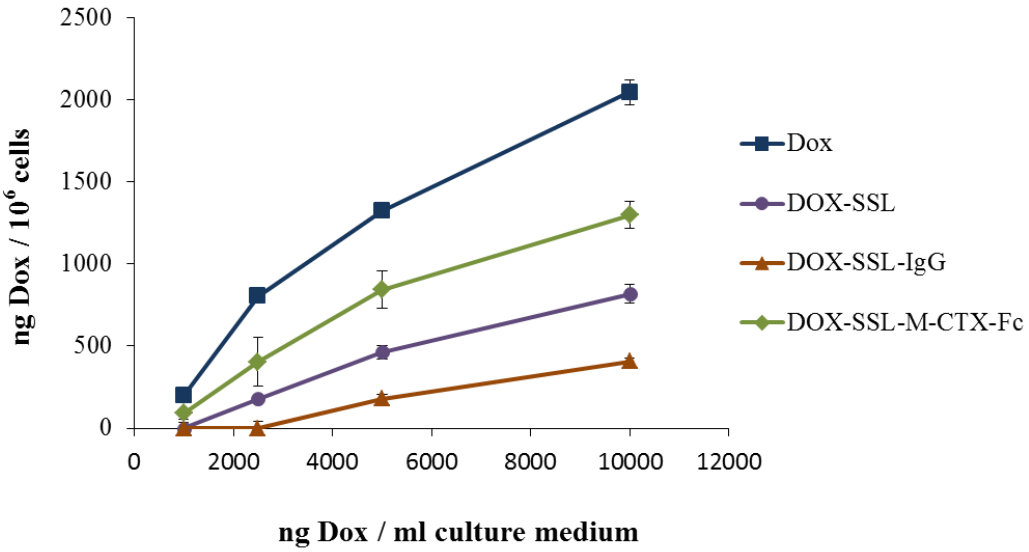

Figure 3: DOX accumulation assay in PANC-1 cells. PANC-1 cells were incubated for 2 h at 37°C with free DOX or DOX encapsulated in different liposomes formulation. DOX was extracted directly from washed PANC-1 cells with acidified isopropanol and measured spectrofluorometrically.

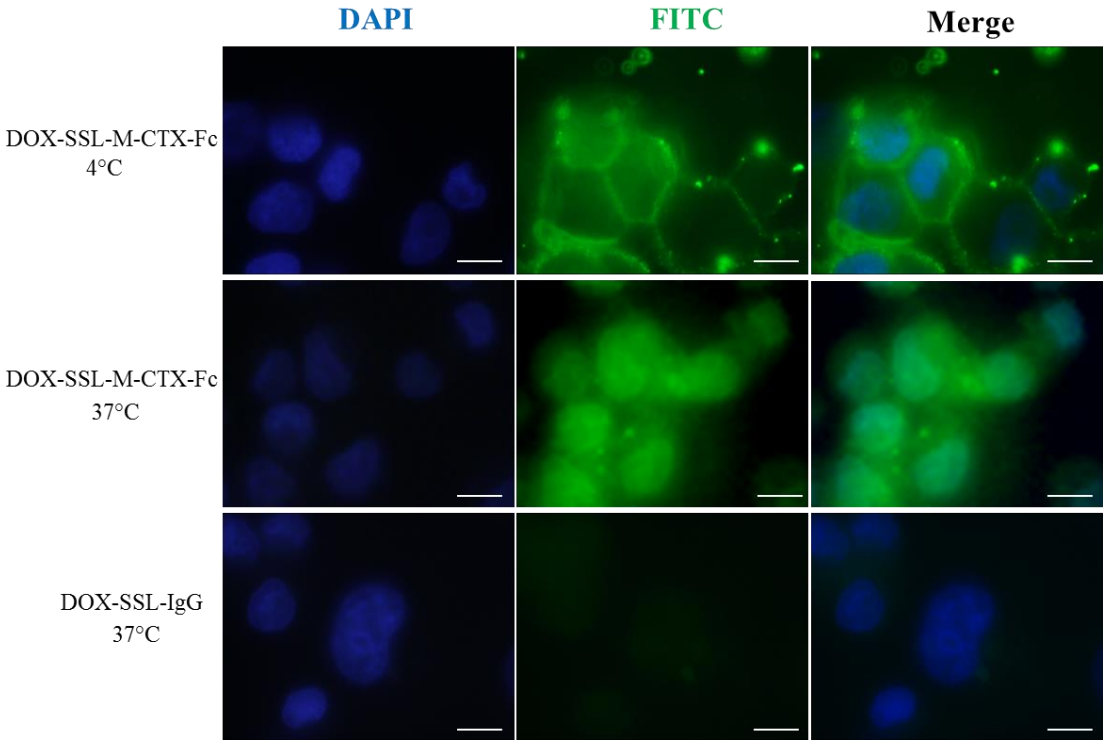

Figure 4: Olympus IX81 microscope observation of M-CTX-Fc or IgG modified DOX-Loading liposomes internalized by PANC-1 cells. PANC-1 cells were treated with DOX-SSL-M-CTX-Fc or DOX-SSL-IgG at 37°C or 4°C and stained with FITC-labeled antihuman IgG antibody.

3.5. *In vivo* antitumor efficacy

In vivo tumor suppression studies were carried out to examine the systemic toxicity and tumor suppression efficiency of different liposome formulations against BALB/c mice bearing PANC-1 cells. After the tumors developed to approximately 50-100 mm^3, the mice were divided into six groups. The designs of *in vivo* antitumor protocol were revealed in

(figure 5A). The progress of tumor growth was observed for 35 days and tumor inhibition efficacy was summarized as a relative tumor volumes normalized by that when liposomes were injected over the time of treatment with different groups, i.e., PBS, M-CTX-Fc, DOX-SSL, combined (DOX-SSL + M-CTX-Fc), DOX-SSL-IgG, and DOX-SSL-M-CTX-Fc. The representative photos of tumor-bearing mice treated by six groups at day 35 were shown in (figure 5B), which provided visible evidence of tumor suppression effect. As shown in figure 4C and figure 4D, it was indicated that DOX-SSL, combined (DOX-SSL + M-CTX-Fc) and DOX-SSL-M-CTX-Fc had superior antitumor efficacy compare with DOX-SSL-IgG. Moreover, DOX-SSL-M-CTX-Fc increased the efficacy because of the higher accumulation in the tumor site. As shown in (figure 5E), the tumor volume of PBS group was increased aggressively. DOX-SSL-IgG and M-CTX-Fc had no effect. The combined treatment (DOX-SSL + M-CTX-Fc) significantly slowed the tumor growth, though they did not completely eliminate the tumors or return to the start level. The M-CTX-Fc modified liposome treatment slowed tumor growth more significantly than either DOX-SSL alone or combined (DOX-SSL+ M-CTX-Fc).

Although the M-CTX-Fc modified liposome treatment did not completely eliminate the tumor, it could maintain the tumor growth at the start level throughout 25 days of the period of treatment. At the end of the test (day 35), the relative tumor volumes of DOX-SSL, combined (DOX-SSL + M-CTX-Fc), and DOX-SSL-M-CTX-Fc were 3.9 ± 0.41 ($P < 0.05$), 3.8 ± 0.35 ($P < 0.05$), and 2.6 ± 0.49 ($P < 0.005$) respectively, compared with the control group of PBS (5.9 ± 0.53). The M-CTX-Fc modified liposomes displayed a stronger inhibiting effect on tumor growth than the others, likely attributing to the combined

processes of passive targeting via EPR effect (27) and the active targeting via receptor mediated endocytosis (28). And this was consistent well with the previous observation in cellular uptake.

However, compared with the obvious differences soon observed between M-CTX-Fc modified liposomes and other groups in cell uptake *in vitro*, it seemed that the significant antitumor activity of DOX-SSL-M-CTX-Fc came late. As we know, the drug molecules distributed in the tumor were only a part of drug molecules in the whole body and drug also eliminated at all time. The efficacy will occur only when enough drug molecules accumulated in tumor cells and this could be achieved only after multiple injections *in vivo*. Additionally, the tumor growth needs time. Usually, the faster the tumors grow, the quicker the difference between control and test group occurs. For all these reasons, it took time from the beginning of treatment to the point that the difference in tumor volume for different treatments could be clearly seen, similar with other studies [29-31].

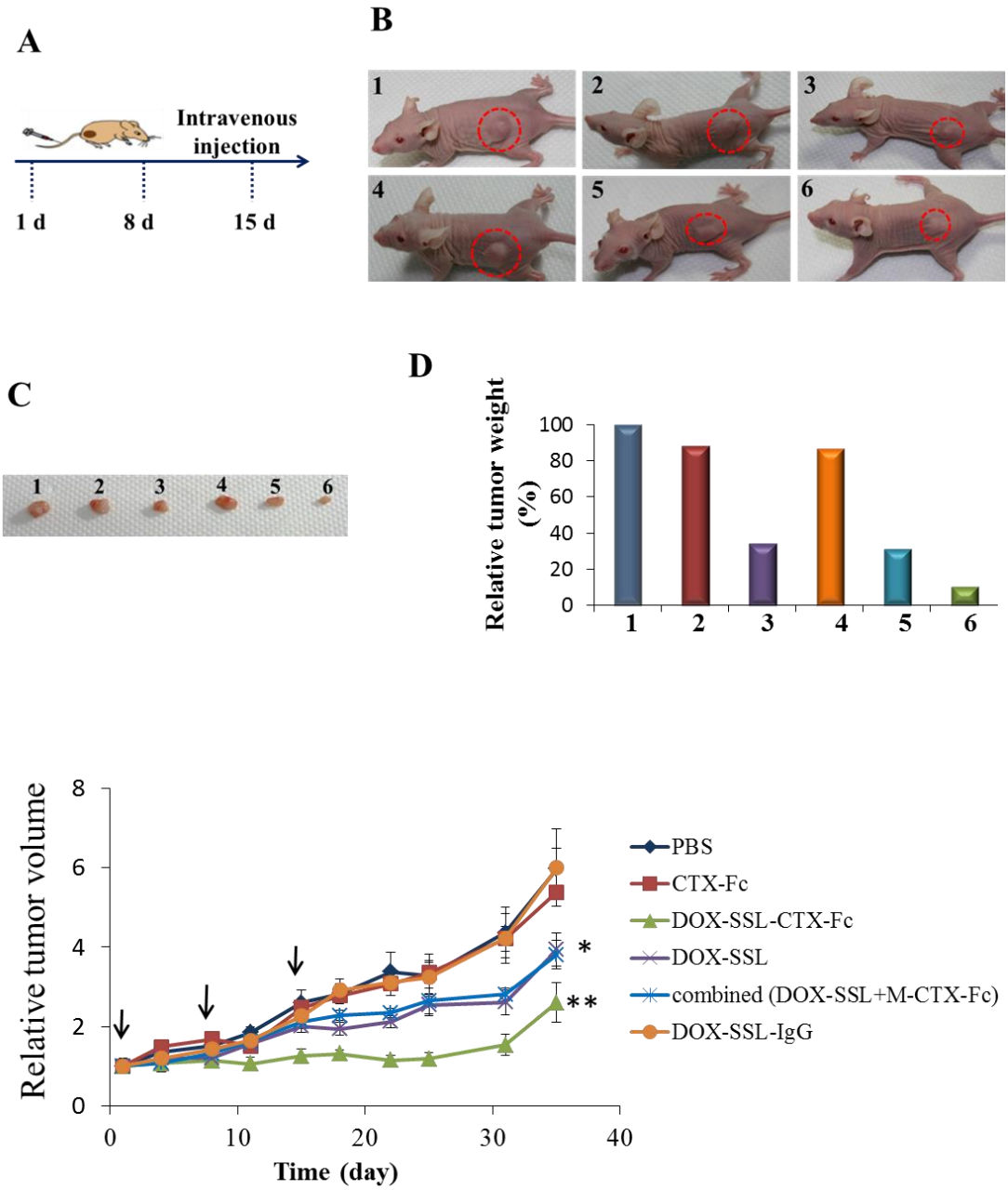

Figure 5: (A) The schematic treatment protocol of mice intravenously injected with (10 mg/kg) DOX-SSL, DOX-SSL-IgG, combined (DOX-SSL+M-CTX-Fc), DOX-SSL-M-CTX-Fc, 1.5 mg/kg M-CTX-Fc, and PBS. Mice were treated every 6 days (day 1, 8, 15). **(B)** Representative photos of

the tumor-bearing mice of six groups with treatments on day 35. 1: PBS, 2: M-CTX-Fc, 3: DOX-SSL, 4: DOX-SSL-IgG, 5: combined (DOX-SSL+M-CTX-Fc), 6: DOX-SSL-M-CTX-Fc. **(C)** photographs of the collected tumor tissues for each treatment group. 1: PBS, 2: M-CTX-Fc, 3: DOX-SSL, 4: DOX-SSL-IgG, 5: combined (DOX-SSL+M-CTX-Fc), 6: DOX-SSL-M-CTX-Fc. (D) Quantitative results of tumor weight excised from the tumor bearing mice sacrificed on day 35. (E) The relative tumor volume changes of the six groups over the course of the treatments (the arrows indicate the injection dates). Values expressed as means ± S.D. Asterisks (∗) denoted statistical significance; ∗, $P < 0.05$; ∗∗ <0.005.

3.6. Systemic Toxicity

For any drug delivery system, Systemic toxicity should be considered to ensure safety even if the system has a good therapy effect. Body weight change was utilized to evaluate the systemic toxicity of the M-CTX-Fc, DOX-SSL, combined (DOX-SSL+M-CTX-Fc), DOX-SSL-IgG, and DOX-SLL-M-CTX-Fc as shown in (figure 6).

The body weight of the mice treated with 10 mg/ml of all formulations of liposomes revealed slight increase from 15 to 19 g (figure 6A), indicating that much less toxicity of various formulation of DOX encapsulated liposomes. No differences in eating, drinking, exploratory behavior, activity and physical features were observed between mice injected with different formulations of liposome and the mice receiving PBS, except the mice receiving DOX-SSL-IgG were lost body weight and activity only after the first dose of injection. However, administration of DOX (10 mg/ kg, tail vein) on day 1, 8, and 15 appeared significant ($P < 0.005$) signs of toxicity, resulting in the pronounced body weight loss in mice (figure 6A and 6B). 25% body weight reduction was observed for DOX treated group due to nonspecific distribution in the body. From these results encapsulation of DOX in liposomes was found remarkably effective to protect mice from toxicity.

This effect of encapsulation was not only recognized in the loss of body weight but also in the survival rate. There were no mice surviving in the group receiving free DOX at dose 10 mg/Kg body weight. The mice did not die when they received DOX-SSL, combined (DOX-SSL+M-CTX-Fc), and DOX-SSL-M-CTX-Fc. As shown in (figure 6B) administration of DOX-SSL, combined (DOX-SSL+M-CTX-Fc), and DOX-SSL-M-CTX-Fc exhibited prolonged survival compared with free DOX. From these results encapsulation of DOX in liposomes was found remarkably effective to protect mice from toxicity.

The systemic toxicity of all formulation of liposomes was further investigated by histopathology assay (figure 7). No apparent toxicity was observed in the tissues from the animal receiving the different formulation of liposomes in comparison to mice receiving PBS. All above results meant that the M-CTX-Fc modified liposome did not cause the unexpected side effects and could be used as safe drug carriers.

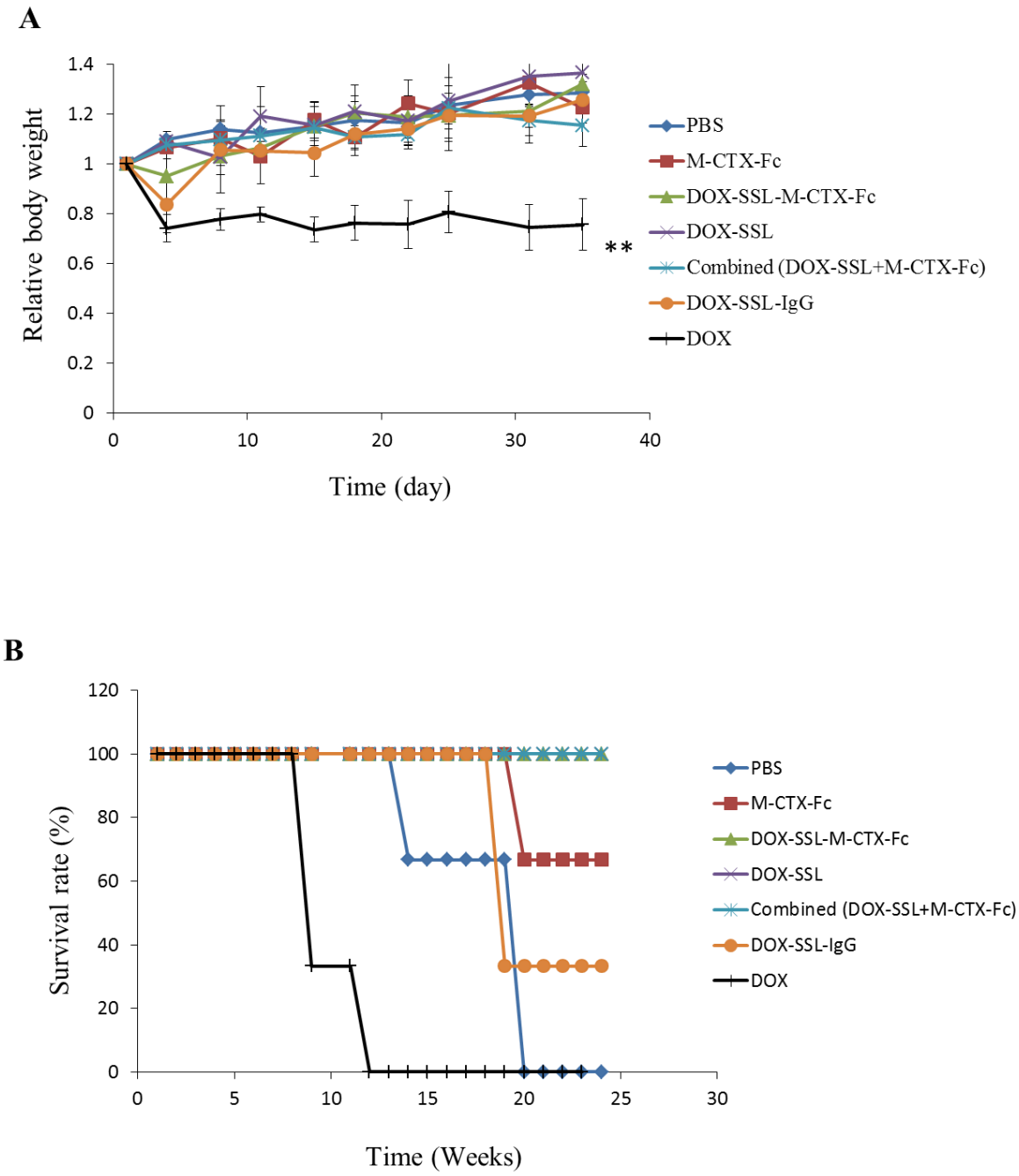

Figure 6: (A) Body weight changes of BALB/c mice bearing PANC-1 tumors during the treatment with free DOX, DOX-SSL, DOX-SSL-IgG, combined (DOX-SSL+M-CTX-Fc),

DOX-SSL-M-CTX-Fc, M-CTX-Fc, and PBS. **(B)** Time profiles for the survival rate of mice during and after treatment with free DOX, DOX-SSL, DOX-SSL-IgG, combined (DOX-SSL+M-CTX-Fc), DOX-SSL-M-CTX-Fc, M-CTX-Fc, and PBS. Survival of mice was followed for up until 5 months

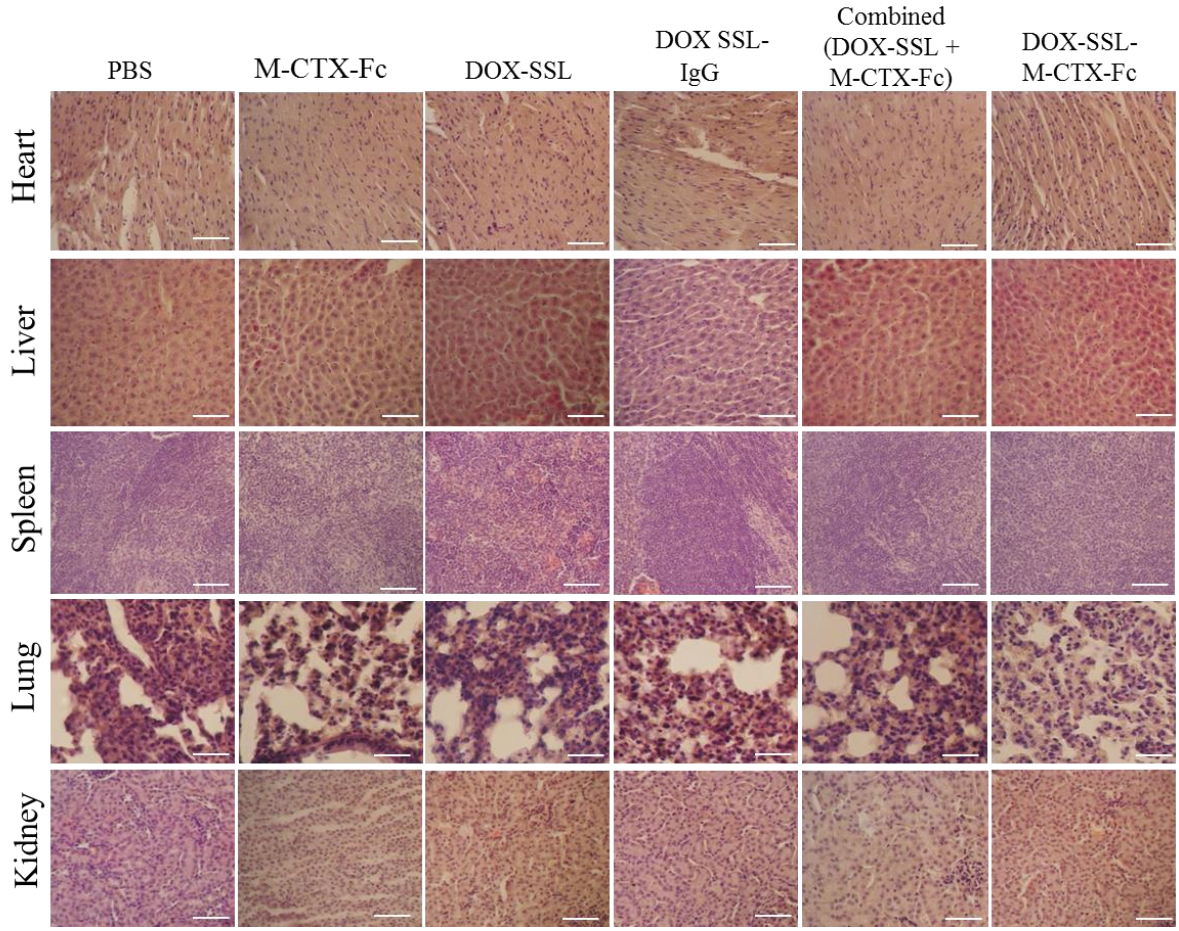

Figure 7: Histopathological examination. (H & E) staining of the main organs after treatment with DOX-SSL, DOX-SSL-IgG, combined (DOX-SSL+M-CTX-Fc), DOX-SSL-M-CTX-Fc, M-CTX-Fc, and PBS.Scale bar 100 μm.

3.7. Immunohistopatology

Recent progress in cancer physiology revealed that tumor growth is closely related to the development of new blood vessels. Then, inhibition of neovascularity is a potent strategy for cancer therapy. Angiogenesis is an invasive process that requires proteolysis of the extracellular matrix and, proliferation and migration of endothelial cells, as well as synthesis of new matrix components. The matix metalloproteinases (MMPs) are a family of extracellular endopeptidases that selectively degrade components of the extracellular matrix. The MMPs are clearly implicated in angioenensis. One of the key proteins on angiogenesis in tumor vessels is membrane type-1 matrix metalloproteinase (MT1- MMP), which is expressed on the neovascularity as well as tumor cells. On the plasma membrane, MT1-MMP cleaved extracellular matrix components such as collagen, laminin, fibronectin and elastin [32-38]. Simultaneously, MT1-MMP activates soluble MMPs (i.e. MMP-2) via its proteolytic activity, which also plays an important role in the degradation of the matrix [32, 34, 36-38]. Tumors expressing MMP-2 have more proliferating vasculature at the tumor-brain interface than MMP-2-negative tumors, implicating a role for MMP-2 stimulation of angiogenesis [39].

Also, PECAM-1/CD31 molecule may be involved in the spread of tumor by interacting with extracellular matrix lysis that results from the tumor cell extravasations and metastasis. In immunohistochemistry, CD31 is used primarily to demonstrate the presence of endothelial cells in histological tissue sections. This can help to evaluate the degree of tumor angiogenesis, which can imply a rapidly growing tumor. As we reported previously that M-CTX-Fc could decrease the release of MMP-2 into the media of PANC-1 cells. So, the effect of non-modified and M-CTX-Fc modified liposome on the angiogenesis process

by immunohistochemical staining for CD31 was examined. (Figure 8A) shows strong and weak expression of CD31 in tumor control and after treatment by DOX-SSL and DOX-SSL-M-CTX-Fc liposome. The CD31 levels suppressed in the DOX-SSL-M-CTX-Fc treatment group (figure 8A). Furthermore, immunohistochemistry of the tumor tissues targeting Ki67 protein, a cellular marker for proliferation showed that the Ki67 level reduced in the DOX-SSL treatment group, compared to the PBS group with the lowest level in DOX-SSL-M-CTX-Fc treatment group (figure 8B).

In fact, administration of the inhibitors for MMP families to the tumor-bearing mouse suppressed the angiogenesis, which resulted in the antitumor effect [40, 41]. Based on previous report, dual targeting of antitumor drugs to the neovascular cells and tumor cells are expected to be excellent strategy for the cancer therapy [42].

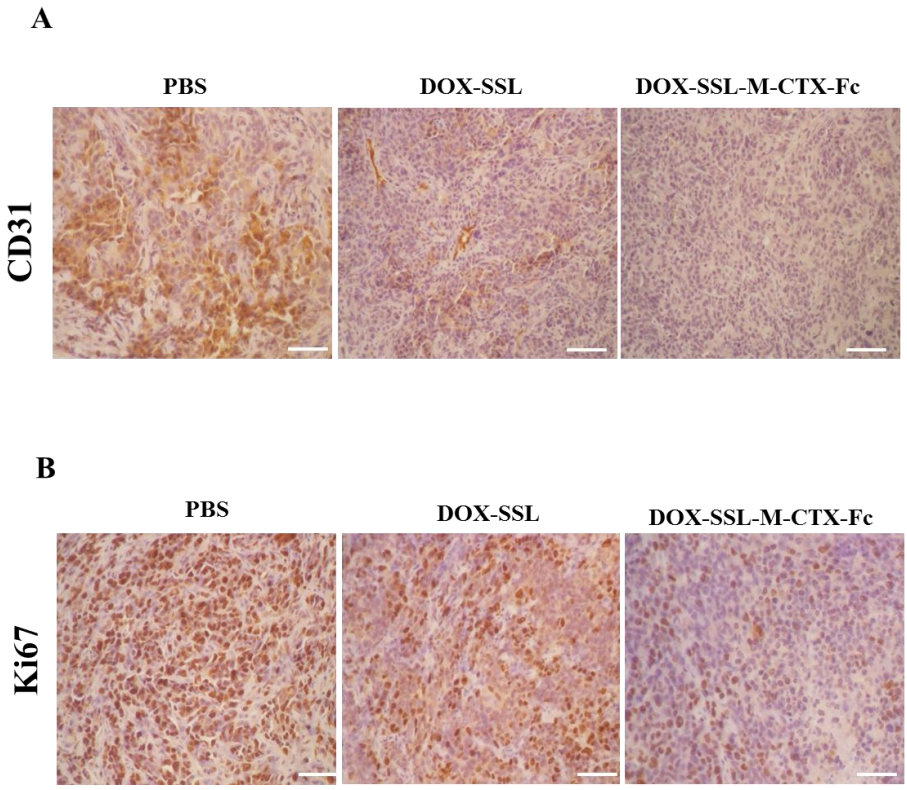

Figure 8: Immunohistochemistry examination (IHC). (A) Showed strong positive for CD31 (brown) in PBS treated mice, weak positive in DOX-SSL, and negative in DOX-SSL-M-CTX-Fc. (B) Showed strong nuclear positivity for Ki67 staining in PBS treated mice and weak nuclear staining in DOX-SSL and DOX-SSL-M-CTX-Fc treated mice.

4. CONCLUTION

DOX loaded M-CTX-Fc modified liposomes was successfully developed by post-insertion method maintaining the targeting ability of M-CTX-Fc liposomes. The M-CTX-Fc modified liposomes exhibited strong enhancement on the cellular uptake against PANC-1 cells. Olympus IX81 microscope confirmed that the DOX-SSL-M-CTX-Fc can move into the interior of PANC-1 cells especially in nuclei while the fluorescent signals is absent in the case of DOX-SSL-IgG. M-CTX-Fc modification could increase the cytotoxicity of liposomes likely due to the high cellular uptake of DOX. The M-CTX-Fc modified liposome treatment slowed tumor growth more significantly than either DOX-SSL alone or combined (DOX-SSL+M-CTX-Fc). DOX-SSL-M-CTX-Fc have the ability to interfere with the expression of CD31 and Ki67 resulting in their reduction and subsequently tumor growth inhibition. The M-CTX-Fc modified liposome did not cause the unexpected side effects and could be used as safe drug carriers. The novel observation that DOX-SSL-M-CTX-Fc can inhibit angiogenesis in the animal model suggests a wider utility of DOX-SSL-M-CTX-Fc in both oncology and other diseases of aberrant neovascularization.

REFERENCES

1. Hariharan D, Saied A, and Kocher HM. Analysis of mortality rates for pancreatic cancer across the world. HPB. 2008; 10 (1): 58–62.
2. Ellenrieder V, Alber B, Lacher U, Hendler SF, Menke A, Boeck W, Wagner M, Wilda M, Friess H, Büchler M, Adler G, and Gress T M. Role of MT-MMPs and MMP-2 in pancreatic cancer progression. Int J Cancer. 2000; 85 (1): 14–20.
3. Liekens S, De Clercq E, Neyts J. Angiogenesis: Regulators and clinical applications. Biochem Pharmacol. 2001; 61 (3): 253–70.
4. Stamenkovic I. Extracellular matrix remodelling: The role of matrix metalloproteinases. J Pathol. 2003, 200 (4): 448–64.
5. Stetler-Stevenson WG. Matrix metalloproteinases in angiogenesis: A moving target for therapeutic intervention. J Clin Invest. 1999; 103 (9): 1237–41.
6. Destouches D, Huet E, Sader M, Frechault S, Carpentier G, Ayoul F, Briand JP, Menashi S, and Courty J. Multivalent Pseudopeptides Targeting Cell Surface Nucleoproteins Inhibit Cancer Cell Invasion through Tissue Inhibitor of Metalloproteinases 3 (TIMP-3) Release. J Biol chem. 2012; 287 (52): 43685–43693.
7. Duffy MJ, Maguire TM, Hill A, McDermott E, O'Higgins N. Metalloproteinases: role in breast carcinogenesis, invasion and metastasis. Breast Cancer Res. 2000; 2 (4): 252−7.

8. DeBin JA, Maggio JE, and Strichartz GR. Purification and characterization of chlorotoxin, a chloride channel ligand from the venom of the scorpion. Am J Physiol. 1993; 264 (2): 361-369.
9. Mamelak AN, and Jacoby DB. Targeted delivery of antitumoral therapy to glioma and other malignancies with synthetic chlorotoxin TM-601. Expert Opin. Drug Deliv. 2007 (2); 4: 175–186
10. Deshane J, Garner CC, and Sontheimer H. Chlorotoxin inhibits glioma cell invasion via matrix metalloproteinase-2. J Biol Chem. 2003; 278 (6): 4135–4144.
11. Soroceanu L, Gillespie Y, Khazaeli MB, and Sontheimer H. Use of chlorotoxin for targeting of primary brain tumors. Cancer Res. 1998; 58 (21): 4871–4879.
12. Lyons SA, O'Neal J, and Sontheimer, H. Chlorotoxin, a scorpion-derived peptide, specifically binds to gliomas and tumors of neuroectodermal origin. Glia. 2002; 39 (2): 162–173.
13. Jacoby DB, Dyskin E, Yalcin M, Kesavan K, Dahlberg W, Ratliff J, Johnson EW, and Mousa SA. Potent pleiotropic anti-angiogenic effects of TM601, a synthetic chlorotoxin peptide. Anticancer Res. 2010; 30 (1): 39-46.
14. Deshane J, Garner CC, Sontheimer H. Chlorotoxin inhibits glioma cell invasion via matrix metalloproteinase-2. J. Biol. Chem. 2003; 278: 4135−44.
15. Shen S, Khazaeli MB, Gillespie GY, Alvarez V. Radiation dosimetry of 131I-chlorotoxin for targeted radiotherapy in gliomabearing mice. J. Neurooncol. 2005; 71 (2): 113−9.

16. Veiseh M, Gabikian P, Bahrami, SB, Veiseh O, Zhang M, Hackman RC, Ravanpay AC, Stroud MR, Kusuma Y, Hansen SJ, Kwok D, Munoz NM, Sze R W, Grady WM, Greenberg NM, Ellenbogen RG, Olson JM. Tumor paint: a chlorotoxin: Cy5.5 bioconjugate for intraoperative visualization of cancer foci. Cancer Res. 2007; 67 (14): 6882−8.
17. Mamelak AN, Rosenfeld S, Bucholz R, Raubitschek A, Nabors LB, Fiveash JB, Shen S, Khazaeli, MB, Colcher D, Liu A, Osman M, Guthrie B, Schade-Bijur S, Hablitz DM, Alvarez VL, Gonda MA. Phase I single-dose study of intracavitary-administered iodine-131-TM-601 in adults with recurrent high-grade glioma. J. Clin. Oncol. 2006; 24 (22): 3644−50.
18. Kasai T, Nakamura K, Vaidyanath A, Chen L, Sekhar S, El-Ghlban S, Okada M, Mizutani A, Kudoh T, Murakami H, and Seno M. Chlorotoxin Fused to IgG-Fc Inhibits Glioblastoma Cell Motility via Receptor-Mediated Endocytosis. J drug deliv. 2012.
19. El-Ghlban S, Kasai T, ShigehiroT, Yin H X, Sekhar S, Ida M, Sanchez CA, Mizutani A, Kudoh T, Murakami H, Seno M. Chlorotoxin-Fc fusion inhibits release of MMP-2 from pancreatic cancer cells. BioMed Res Int. 2014; 2014: 152659.
20. Mendonça LS, Firmino F, Moreira JN, Pedroso de Lima, MC and Simões S. Transferrin receptor-targeted liposomes encapsulating anti-BCR-ABL siRNA or asODN for chronic myeloid leukemia treatment. Bioconjug Chem. 2010; 21(1): 157–168.

21. Moreira JN, Ishida T, Gaspar R and Allen TM. Use of the post-insertion technique to insert peptide ligands into pre-formed stealth liposomes with retention of binding activity and cytotoxicity. Pharm Res. 2002; 19 (3): 265–269.
22. Chambers SK, Hait WN, kacinski BM, Keyes SR. and Handschumacher RE. Enhancement of anthracycline growth inhibition in parent and multidrug-resistant Chinese hamster ovary cells by cyclosporin A and its analogues. Cancer Res. 1989; 49 (22): 6275-6279.
23. Riezman H, Woodman PG, Van Meer G, Marsh M. Molecular mechanisms of endocytosis. Cell. 1997; 91(6): 731–738.
24. Allen TM, Cheng WW, Hare JI, Laginha KM. Pharmacokinetics and pharmacodynamics of lipidic nano-particles in cancer. Anticancer Agents Med. Chem. 2006; 6 (6): 513–523.
25. Xu Z, Gu W, Huang J, Sui H, Zhou Z, Yang Y, Yang Z, Li Y. In vitro and in vivo evaluation of actively targetable nanoparticles for paclitaxel delivery. Int. J. Pharm. 2005; 288 (2): 361–368.
26. Moreira JN, Gaspar R, Allen TM. Targeting Stealth liposomes in a mutine model of human small cell lung cancer. Biochim. Biophys. Acta. 2001; 1515 (2): 167–176.
27. Gabizon AA. Selective tumor localization and improved therapeutic index of anthracyclines encapsulated in long-circulating liposomes. Cancer Res. 1992; 52 (4): 891–896.
28. Torchilin VP. Passive and active drug targeting: drug delivery to tumors as an example. Handb. Exp. Pharmacol. 2010; 197: 3–53.

29. Nie H, Fu Y, Wang CH. Paclitaxel and suramin-loaded core/shell microspheres in the treatment of brain tumors. Biomaterials. 2010; 31 (33): 8732–8740.

30. Labussière M, Aarnink A, Pinel S, Taillandier L, Escanyé JM, Barberi-Heyob M, Bernier-Chastagne V, Plénat F, Chastagner P. Interest of liposomal doxorubicin as a radiosensitizer in malignant glioma xenografts. Anticancer Drugs. 2008; 19 (10): 991–998.

31. Niu G, Driessen WH, Sullivan SM, Hughes JA. In vivo anti-tumor effect of expressing p14ARF-TAT using a FGF2-targeted cationic lipid vector. Pharm. Res. 2011; 28 (4): 720–730.

32. Knauper V, Will H, Lopez-Otin C, Smith B, Atkinson SJ, Stanton H, Hembry RM, Murphy G. 1996. Cellular mechanisms for human procollagenase-3 (MMP-13) activation. Evidence that MT1-MMP (MMP-14) and gelatinase a (MMP-2) are able to generate active enzyme. J. Biol. Chem. 1996; 271 (29): 17124–17131.

33. Noel A, Santavicca M, Stoll I, L'Hoir C, Staub A, Murphy G, Rio MC, Basset P. Identification of structural determinants controlling human and mouse stromelysin-3 proteolytic activities. J. Biol. Chem. 1995; 270 (39): 22866–22872.

34. Ohuchi E, Imai K, Fujii Y, Sato H, Seiki M, Okada Y. Membrane type 1 matrix metalloproteinase digests interstitial collagens and other extracellular matrix macromolecules. J. Biol. Chem. 1997; 272 (4): 2446–2451.

35. Pei D, Majmudar G, Weiss SJ. Hydrolytic inactivation of a breast carcinoma cell-derived serpin by human stromelysin-3. J. Biol. Chem.1994; 269: 25849–25855.

36. Pei D, Weiss SJ. Transmembrane-deletion mutants of the membrane-type matrix metalloproteinase-1 process progelatinase A and express intrinsic matrix-degrading activity. J. Biol. Chem. 1996; 271 (15): 9135–9140.
37. Sato H, Takino T, Okada Y, Cao J, Shinagawa A, Yamamoto E, Seiki M. A matrix metalloproteinase expressed on the surface of invasive tumour cells. Nature. 1994; 370 (6484): 61–65.
38. Strongin AY, Collier I, Bannikov G, Marmer BL, Grant GA, Goldberg GI. Mechanism of cell surface activation of 72-kDa type IV collagenase. Isolation of the activated form of the membrane metalloprotease. J. Biol. Chem. 1995; 270 (10): 5331–5338.
39. Rojiani MV, Alidina J, Esposito N, Rojiani AM. Expression of MMP-2 correlates with increased angiogenesis in CNS metastasis of lung carcinoma. Int J Clin Exp Pathol. 2010; 3 (8): 775-81.
40. Maekawa R, Maki H, Yoshida H, Hojo K, Tanaka H, Wada T, Uchida N, Takeda Y, Kasai H, Okamoto H, Tsuzuki H, Kambayashi Y, Watanabe F, Kawada K, Toda K, Ohtani M, Sugita K, Yoshioka T. Correlation of antiangiogenic and antitumor efficacy of N-biphenyl sulfonylphenylalanine hydroxiamic acid (BPHA), an orally active, selective matrix metalloproteinase inhibitor. Cancer Res. 1999; 59 (6): 1231–1235.
41. Nelson NJ. Inhibitors of angiogenesis enter phase III testing. J. Natl. Cancer Inst. 1998; 90(13): 960–963.

42. Maeda N, Takeuchi Y, Takada M, Sadzuka Y, Namba Y, Oku N. Anti-neovascular therapy by use of tumor neovasculature-targeted longcirculating liposomes. J. Control. Release. 2004; 100 (1): 41–52.

LIST OF PUBLICATIONS

(1) Chlorotoxin-Fc Fusion Inhibits Release of MMP-2 from Pancreatic Cancer Cells.

Samah El-Ghlban, Tomonari Kasai, Tsukasa Shigehiro, Hong Xia Yin, Sreeja Sekhar, Mikiko Ida, Anna Sanchez, Akifumi Mizutani, Takayuki Kudoh, Hiroshi Murakami, and Masaharu Seno.

BioMed Research International. Volume 2014 (2014), Article ID 152659.

http://dx.doi.org/10.1155/2014/152659.

(2) Chlorotoxin fused to IgG inhibits glioblastoma cell motility via receptor-mediated endocytosis.

Tomonari Kasai, Keisuke Nakamura, Arun Vaidyanath, Ling Chen, Sreeja Sekhar, Samah EL-Ghlban, Masashi Okada, Akifumi Mizutani, Takayuki kudoh, Hiroshi Murakami, and Masaharu Seno. Journal of Drug delivery. Volume 2012, Article ID 975763.

http://dx.doi.org/10.1155/2012/975763

ORAL AND POSTER PRESENTATIONS

(1) Chlorotoxin-Fc Fusion Inhibits Release of MMP-2 from Pancreatic Cancer Cells.

Samah EL-Ghlban, Tomonari Kasai, Akifumi Mizutani, Hiroshi Murakami, and Masaharu Seno.The Molecular Biology Society of Japan**,** The 36th Annual Meeting of Molecular Biology Society of Japan. 2013.12.04.

(2) Chlorotoxin-Fc Fusion Inhibits Release of MMP-2 from Pancreatic Cancer Cells.

Samah EL-Ghlban, Tomonari Kasai, Akifumi Mizutani, Hiroshi Murakami, and Masaharu Seno.The 7th international Symposium for future technology Creating Better Human Health and Society. 2014. 2. 7.

Acknowledgements

First of all I should express my deep express to *ALLAH*, without great blessing I should have never accomplished this work.

Foremost, I would like to express my sincere gratitude to my supervisor *Prof. Masaharu Seno* for the continuous support of my Ph.D study and research, for his patience, motivation, enthusiasm, and immense knowledge. His guidance helped me in all the time of research and writing of this thesis. I could not have imagined having a better supervisor and mentor for my Ph.D study. Thank you seno sensie for letting me fulfill my dream of being a student in your lab.

I am grateful to *prof. Takashi Sera and Prof. Takashi Ohtsuki* for their kind reviewing my thesis.

I would like to express my sincere gratitude to *Dr. Tomonari Kasai*. I am not sure that this project would have been possible without you. You were always available for my questions and you were positive and gave generously of your time and vast knowledge.

I would like to thanks *Dr. Hiroshi Murakami and Dr. Akifumi Mizutani* for their continuing support and motivation throughout the work. I would like to extend my sincere gratitude to *Dr. Junko Masuda* and *Takayuki Kudoh* for their support and motivation.

The special gratitude should be given to my *Prof. Ibrahim EL-Sayed*, EL-Menofiya University, Egypt, for providing me the opportunity to study in Okayama University.

Furthermore, the special gratitude should be given to *Ms. Mami Asakura* for her warmth and kindness to me during my whole study in japan.

I also need to express my gratitude to a group of supportive friends and extended family who never stopped trying to understand just what it was I was studying and were always there when I need to inject a little humor into my life.

I gratefully achnowledge the funding received towards my PhD from MEXET (Ministry of Education, Culture, Sports, Science, and Technology)

I am grateful for my family especially, my father and my mother. Their loves encouraged me to work hard and to continue pursuing the Ph.D. project abroad. Most of all, thank you to a sweet *husband* who has endured the most stressful period of completing this degree right by my side.

I must acknowledge my son and my best friend, *Yousef*, without whose love, I would not have finished this thesis.

Samah EL-Ghlban
Okayam university